AES 4011-10 Additional thesis project: An experiment on low-cost RTK GNSS with short baseline performance

Menglin Pang
Civil Engineering and Geoscience
TU Delft
4/5/2017

AES 4011-10 Additional thesis project: An experiment on low-cost RTK GNSS with short baseline

Menglin Pang
Civil Engineering and Geoscience
TU Delft
4/5/2017

Summary

This report first elaborates on an experiment to evaluate the performance of single frequency base station performance along with baseline. The system is deployed on a single frequency base station, and low-cost antenna in both and base and rover setup. The experiment is based on taking measurements on six control points, which are selected by varying simple topographic information and baseline length difference, by connecting to the single frequency base station. To have better evaluation of the performance of six control points, three sets of data, fix, float and all the measurements are divided and a simplified outlier detection model is employed to process the position estimates per control point. Finally, combine the results extracted from each control points to see the baseline length influence.

The experiment is conducted on basis that the precise position of base station is known. While users may construct their base station with unknown location. The document also includes several methods on how to determine an unknown base station position by using NETPOS product, and compare advantages and disadvantages internally, by which user can choose the method accordingly. In the last part of the document, a detail instruction on implementation of low-cost base station and rover setup in the previous experiment, including the needed hardware setup and software configurations, is provided for the potential users.

Table of Contents

Summary i

Introduction 1

Part I 2

- Working single baseline setup 2
- Deployment in the experiment 3
- Data preparation 4
- Model 4
- Method 6
- Result 7
- Conclusion and discussion 16

Part II 16

- NETPOS product 16
- Approaches 17
- Summary 18

Part III 19

Hardware preparation 19

Software configuration 20
Conclusions 26

Appendix A: Plots for each control point 27

Appendix B: Satellite numbers in the view for each session 53

Appendix C: TTSF for each session 54

Acknowledgement 55

References 56

Introduction

Current GNSS network of RTK technique make use of geodetic grade multi-frequency GPS receivers and allows users to have sub-centimeter accuracy (Chen & Gao, 2005). However, only professional users can have access to this kind of high-accuracy solutions due to its high cost. To meet the growing needs from wider group of single-frequency receiver users, and at the meantime, guarantee the price low enough, a dense reference network made up by single frequency RTK would become feasible, owing to the availability of more satellites and signals (Sneeuw, Novák, Crespi, & Sansó, 2012).

The RTK system requires at least two RTK capable receivers one base station and one or more rovers, where the base stations are placed on an accurate known location and rover on the location to determine, and a data link communication via wireless datalink between the receivers. The base station will provide corrections for the rover observation. When the base station and the rover observing the satellite geometry at the same time, the two receivers of base and rover share the same clock errors and partially satellite errors, therefore, fix solutions are obtained. At the meantime, to obtain the high level of accuracy, the base station must be carefully selected to obtain good quality of measurements and very precisely set up at a known location, and deploy the reference station in a dense pattern to reach centimeter accuracy, since a shorter baseline can have negligible errors caused by atmospheric influence, what's more, the reference information provided by NTrip, which mostly derived by virtual reference station or master auxiliary concept, is most cost-effective method for single-frequency base station networks (Stempfhuber & Buchholz, 2011)

Feasibility and application of such a dense single-frequency base station network has aroused interest from many researchers worldwide, multiple studies have been employed under this subject. (Sneeuw et al., 2012) analyze the single frequency RTK positioning by exploiting ambiguity resolution performance under different scenarios, and they found the solution only feasible within 5 km baselines. (Takasu & Yasuda, 2004) evaluate the performances with combination of various antenna and receivers, they conclude the difference of solutions between the multi-frequency hardware and single frequency ones is comparable in carrier-phase performances. (Takasu & Yasuda, 2009) also support that performance from single-frequency receivers with good antenna processes by RTKLIB is quite promising. Further, (Pesyna, Heath, & Humphreys, 2015) evaluate the positioning accuracy with a smartphone-quality GNSS antenna, and they point out that the poor quality of phase center and axial ratio, intrinsically the antenna size, leads to less power that the smartphone-grade antenna can capture, and this contribute to greater variations of ambiguity resolution and longer time to obtain it with good quality.

Although it is well accepted that the of single-frequency base station can have good measurements within a shorter baseline, how accuracy will vary within this short baseline? Are they have the same performance in all directions? Will the location of control point have an effect on measurements? How much it will affect the quality of the measurements? In this project, we will explore the answers to these questions by deploying a simple experiment with a single-frequency base station, and connect the base station and rover with cheap antennas, by varying the baseline length of the different rover locations, and in the end, find the feasibility of this application, also provide suggestions for potential users accordingly.

Part I: experiment set-up and evaluation

Working single baseline setup:

The experiment is an exploration of single-frequency reference station feasibility on a short baseline regime, so the location of selected control points varies according to their baseline length. However, the satellite visibility also has a strong impact on positioning accuracy, which will affect the time to static fix (TTSF) of each observation, so we also decide to include simple topographic information (building-surrounded and open area) and swap measuring time to explore the quality of different testing results.

Based on the ideas above, 6 control points are selected in total, distributed by a distance interval of approximately 1 km from the single frequency station, point 3 and 4 are located in proximity of low and high buildings respectively, and the rest of the control points are located in the open area (see figure 1), to have an understanding of the influence of baseline length on measurements quality and the initialization time of getting static fix solutions.

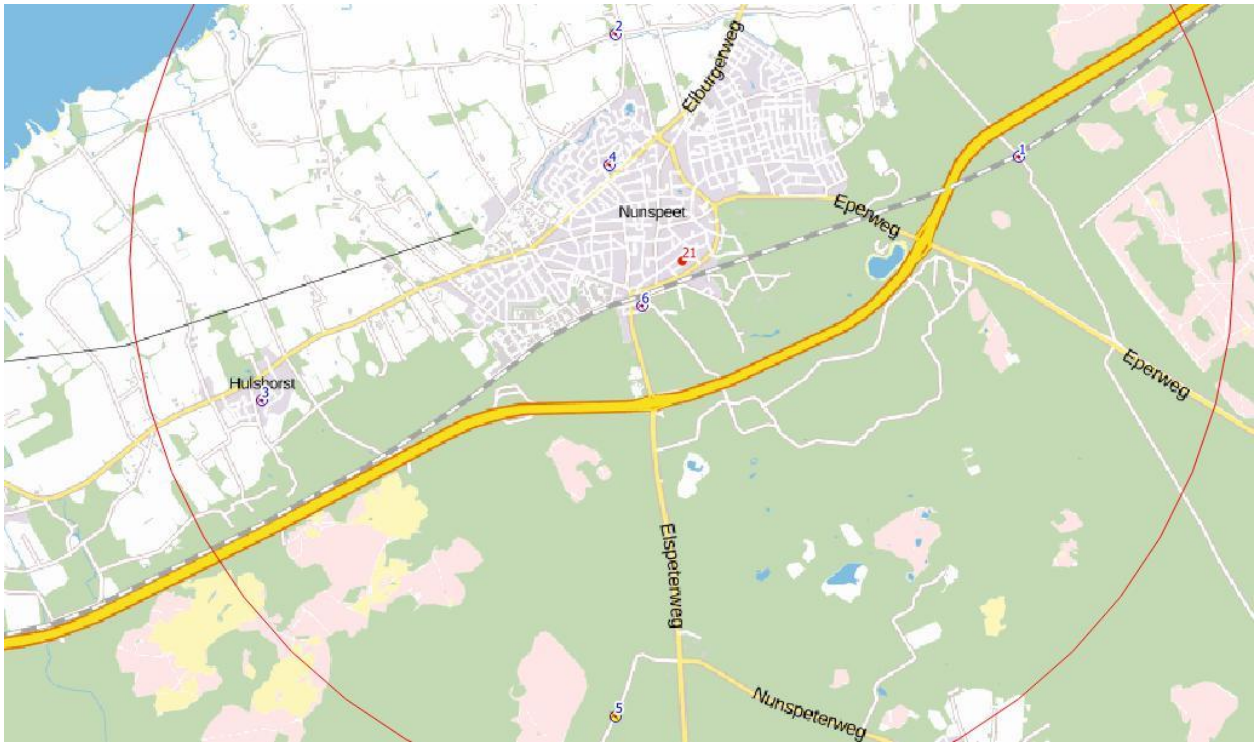

Figure 1. Overview plot of six control points in the experiment

For the experiment, these data are measured:

1. Baseline length to the base station by each control point.
2. The ground truth coordinates for the control points and the base station.
3. Enough observations per control point.

Deployment in the experiment

The idea is based on *Kadaster* NETPOS One concept, detail introduction and configuration can be referenced to Part III. The system consists of a base station setup and a rover setup, the former one locations on precisely known coordinates and the later one locates on the unknown position. The location of base station is very important, which will be directly influenced the available satellite numbers when taking measurements, since the signal can be affected by the surroundings. The first attempt on single frequency base station location selection is not good, probably because of the chimney that blocks the satellite signal. Then we move it to another site of the roof, and this time, when checking the SNR plot in RTKNAVI windows, the performance is improved but still not very stable, the number of satellites with good signal is very few, which will contribute to more float measurements. This probably relies on the satellite visibility or the weather conditions on that day. What's more, TTSF also varies due to the variation of baselines and its surroundings, its value, the time the observations stay fixed, is unstable either. Sometimes it will last 5 minutes, sometimes it is too short to take several fix measurements, this results in less number of continuous fix measurements and a lot of random fix measurements.

After setting up the base station, we continue with taking measurements in each control points**.** The plan is to take two sets of measurements, by changing the measuring time from 9 am – 5 pm to before 9 am or after 6 pm. By taking measurements under different satellite visibility and geometry, we can have more reliable measurements. The practical experiment takes 5 days in total. In the first two days, we take measurements on control point 1-4, and this first set of measurements, which are the 1-5 sessions in control point 1-4, we found that the measurements have less fix measurements by the SNR plot in RTKNAVI. Then another set of measurements in control point 1, 4 and 5 is taken early in the morning and in the evening. By changing the measuring time, we hope the available satellite numbers will grow, and therefore have more fix measurements. Although the measurements in one control point are not taken continuously in time especially for control point 1-4, in the later processing procedure, we treat all the measurements with no difference in time.

In summary, for control point 2 and 3, each of them has 5 sessions of measurements; for control point 1 and 4, they have 9 sessions of observations for each, and due to the poor number of fix solutions for the first five sessions, the later five are taken by changing the measuring time; the rest 2 locations, control point 5 and 6 have 9 sessions that are all taken during changing measuring time. For each session, it takes 15 minutes to observe with measuring frequency 1 Hz. In the end, control point 2 and 3 have at least 4000 measurements, and control point 1, 4, 5 and 6 have more than 7000 measurements.

The base station setup in the experiment is shown in Fig. 2, on the left: the final base station locates on a roof, with no obvious tall obstacles surrounding it. The antenna attaching on the base station is a low-cost one. Rover setup in the experiment in one the right hand-side of Fig. 2: the antenna is set on top of the rod, this is to reduce the multipath effect and to get strong signal, the user should take down the rover height difference for the later correction in Up direction. Instead of using mobile phone in the rover setup, we decide to use tablet with RTKLIB 2.4.2v to get more stable position estimates. When taking the measurements, we can have a rough check of the dataset by looking into the RTKNAVI windows. Then after taking measurements for 15 minutes for one session, save them in 'ENU-baseline' format.

Figure 2. Base station (left) and rover setup of control point 1(right) pictures

Data preparation

In the experiment, baseline estimates from all sessions from one control point is combined as the input of the model. Although the fix solutions have higher accuracy, but factors such as base station coordinate accuracy, satellite visibility, environmental factors will greatly reduce the number of observations. Therefore, all measurements are considered in one control point. While the computation for TTSF is determined by the start time of at least 100 continuous fix solutions from each session, this step is to avoid fake TTSF that resulted from discrete fix solutions and to guarantee that there are enough measurements (100) in after time to get fix.

In each control point, evaluations are conducted based on fix, float and all measurements, to explore the statistics in detail. And the data is divided by selection of quality flag: when quality flag = 1, we will have the fix measurements; if quality flag = 2, we will have the float measurements.

Model

Because we combine all the data in one control point, there are some invalid measurements, such as the measurements before the solutions get fix and discrete fix/float solutions, will need to

be filtered. Therefore, we use a simple model to process the data for each control point. The idea is to apply least square adjustment to observations in order to have the optimal solution in all three directions, then to compute the residuals with the observation in order to detect blunders by w-test values. The model assumes that the errors in the observations form normal distribution, therefore, the blunders are filtered when if falls out of the 95% of normal distribution confidence interval. The model is presented as:

$$\begin{pmatrix} N' \\ E' \\ U' \end{pmatrix} = \begin{pmatrix} 1 & 0 & 0 \\ 0 & 1 & 0 \\ 0 & 0 & 1 \end{pmatrix} \begin{pmatrix} N \\ E \\ U \end{pmatrix} + \epsilon$$

N', E', U' here are the observations, which we obtained from RTKLIB solution; N, E, U are the estimations; ϵ is the noise in the model. And the variance-covariance matrix for the observation term in the model:

$$Q_{yy} = \begin{pmatrix} \begin{pmatrix} Q_{NN} & \cdots & 0 \\ \vdots & \ddots & \vdots \\ 0 & \cdots & Q_{NN} \end{pmatrix} & \begin{pmatrix} Q_{NE} & \cdots & 0 \\ \vdots & \ddots & \vdots \\ 0 & \cdots & Q_{NE} \end{pmatrix} & \begin{pmatrix} Q_{NU} & \cdots & 0 \\ \vdots & \ddots & \vdots \\ 0 & \cdots & Q_{NU} \end{pmatrix} \\ \begin{pmatrix} Q_{EN} & \cdots & 0 \\ \vdots & \ddots & \vdots \\ 0 & \cdots & Q_{EN} \end{pmatrix} & \begin{pmatrix} Q_{EE} & \cdots & 0 \\ \vdots & \ddots & \vdots \\ 0 & \cdots & Q_{EE} \end{pmatrix} & \begin{pmatrix} Q_{EU} & \cdots & 0 \\ \vdots & \ddots & \vdots \\ 0 & \cdots & Q_{EU} \end{pmatrix} \\ \begin{pmatrix} Q_{UN} & \cdots & 0 \\ \vdots & \ddots & \vdots \\ 0 & \cdots & Q_{UN} \end{pmatrix} & \begin{pmatrix} Q_{UN} & \cdots & 0 \\ \vdots & \ddots & \vdots \\ 0 & \cdots & Q_{UN} \end{pmatrix} & \begin{pmatrix} Q_{UU} & \cdots & 0 \\ \vdots & \ddots & \vdots \\ 0 & \cdots & Q_{UU} \end{pmatrix} \end{pmatrix}$$

To guarantee the Q_{yy} in the model precise enough, its components are computed only by fix solutions from all data in a control point which can be selected by choosing flag = 1. The covariance values are computed by:

$$\begin{pmatrix} Q_{NN} & Q_{NE} & Q_{NU} \\ Q_{EN} & Q_{EE} & Q_{EU} \\ Q_{UN} & Q_{UE} & Q_{UU} \end{pmatrix} = \frac{1}{N-1} \begin{pmatrix} N_1 - \bar{N} & \cdots & N_i - \bar{N} \\ E_1 - \bar{E} & \cdots & E_i - \bar{E} \\ U_1 - \bar{U} & \cdots & U_i - \bar{U} \end{pmatrix} \begin{pmatrix} N_1 - \bar{N} & E_1 - \bar{E} & U_1 - \bar{U} \\ \vdots & \vdots & \vdots \\ N_i - \bar{N} & E_i - \bar{E} & U_i - \bar{U} \end{pmatrix}$$

Where N is the number of measurements, $\bar{N}, \bar{E}, \bar{U}$ are their means. Then we apply w-test is to identify the blunders in the estimation. The w-test value is also defined as normalized residual as follows, conforming normal distribution with a zero-mean, and the threshold for its 95% confidence interval is [-1.96,1.96]:

$$\mathrm{w_i} = \frac{\hat{e}_i}{\hat{\sigma}_{e_i}}$$

Where $\hat{e}_i$ is the residual from the observation and estimation, and $\hat{\sigma}_{e_i}$ is its standard deviation, is computed by taking the square root of the diagonal values of $\mathrm{Q}_{\hat{e}\hat{e}}$, the equations are shown as follows:

$$\mathrm{Q}_{\hat{e}\hat{e}} = Q_{yy} - \mathrm{Q}_{\hat{y}\hat{y}}$$

$$\mathrm{Q}_{\hat{y}\hat{y}} = \mathrm{A}\left(\mathrm{A^T Q_{yy}^{-1} A}\right)^{-1} A^T$$

The A matrix here is the identity matrix on the right hand side of the model equation. During the experiment, the computation for each control points is very large since there are several thousands of measurements in one control points. To reduce the computational effort, we made some simplifications when running the model. First, we compute the estimation by taking the means. Second, we find that the $\mathrm{Q}_{\hat{e}\hat{e}}$ values are very close to Q_{yy} and the diagonal values are much larger than the rest. So in the application, we simplified the $\sigma_{\widehat{e_i}}$ by taking the square root of the

diagonal values of observations covariance matrix to reduce the computational effort. Thus, the equation for computing w-test is changed into:

$$w_i = \frac{\hat{e}_i}{\sqrt{diag(Q_{yy_i})}}$$

The blunder is detected by finding the maximal absolute value in *w*, if it is out of the 95% confidence interval or not. Once the blunder is found, discard the whole measurement (N, E and U) and the corresponding element in covariance matrix, and run the procedure again. The final solution will be reached after several iterations until there is no outliers detected. Once the raw data is cleaned, that is, there is no outliers in the data, we can use them to compare with the ground truth solution again to see how the statistics change.

Method

This session is to introduce the statistics that we use to evaluate the data performance by comparing the precision, bias and the number of blunders removed to obtain the cleaned data. To have a good evaluation, the statistics are computed both before and after running the model, to check how the procedure changes the data performance. Meanwhile, for better understanding of the baseline influence, TTSF is also considered in evaluation.

Because we are only interested in statistics in 'ENU-baseline' format, conversions between different coordinates format are needed. The ground truth coordinates are given in spherical coordinates and the measurements are recorded in 'ENU-baseline' format, conversions are needed to have the bias under local CRS. A simple procedure map between the conversions:

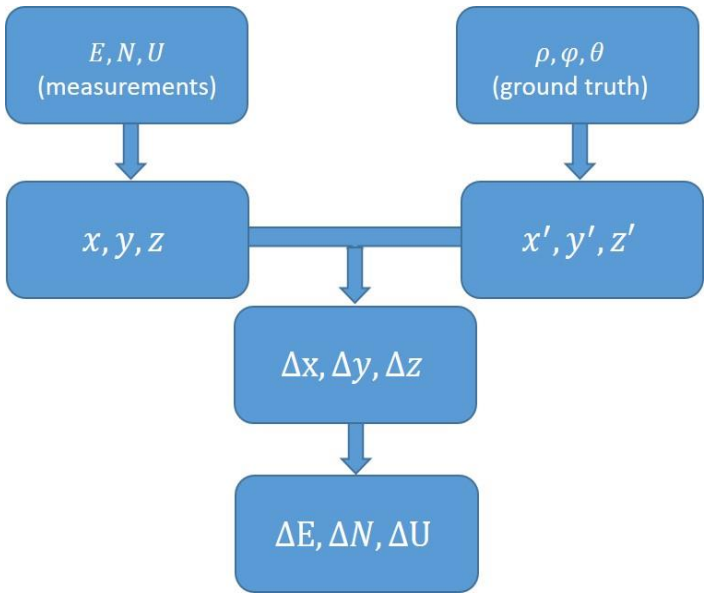

Figure 3. Data conversion map between different format.

Some statistics used in evaluation:
Bias is computed by:

$$\bar{\mu} = \frac{\sum_{i=1}^{n}(NEU_i - NEU_0)}{n} = \frac{\sum_{i=1}^{n}\Delta\widehat{NEU}_i}{n} = \frac{\sum_{i=1}^{n} f(\Delta \mathrm{XYZ_i})}{n} = \frac{\sum_{i=1}^{n} f(\mathrm{XYZ_i} - \mathrm{XYZ_0})}{n}$$

Standard deviation of the observations:

$$\sigma = \sqrt{\frac{\sum_{i=1}^{n}(NEU_i - \overline{NEU})^2}{n}}$$

RMS is the presented as:

$$M = \sqrt{\frac{\sum_{i=1}^{n}\left(\Delta\widehat{NEU}_i\right)^2}{n-1}} = \sqrt{\frac{\sum_{i=1}^{n}(f(\Delta \mathrm{XYZ_i}))^2}{n-1}} = \sqrt{\frac{\sum_{i=1}^{n}\left(f(\mathrm{XYZ_i} - \mathrm{XYZ_0})\right)^2}{n-1}}$$

Where *f* is the function *xyz2neu*; $NEU_i$is the measurements in ENU-baseline format, $\overline{NEU}$ is the mean of NEU; NEU_0 is converted control point coordinates; $\mathrm{XYZ_i}$ is measurements in *ECEF* format; XYZ_0 is the ground truth coordinate in *ECEF* format; *n* is the number of measurements.

Result

For each control point, the fix, float and all measurements are evaluated separately. Therefore, for each part, times series, scatter plot and histogram in three directions before and after removing outliers are included. Here is an example of result for control point 2 all solutions. For the rest of the solutions, please find their figures in the Appendix A.

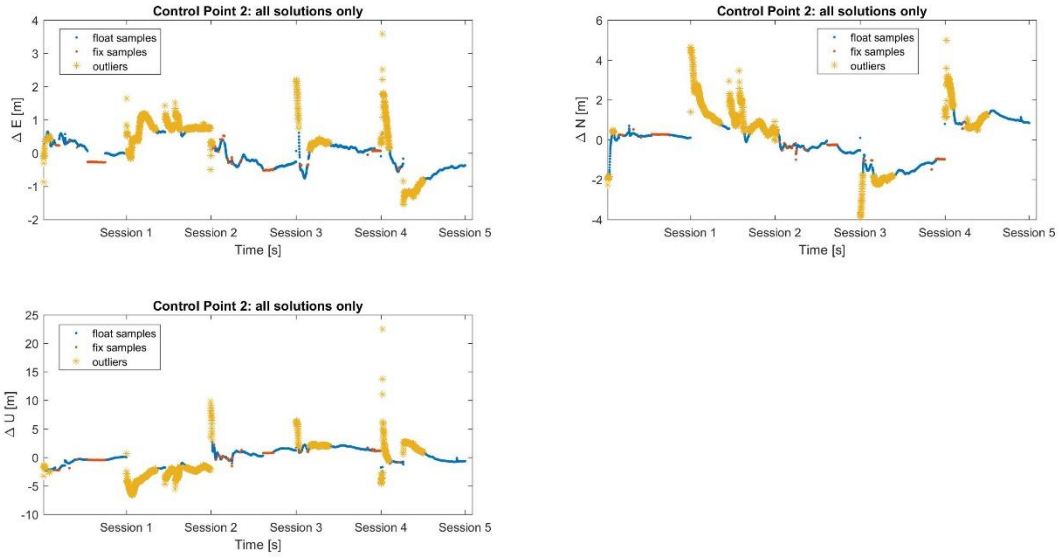

Figure 4. Time series of control point 2 all measurements.

The example time series in three directions contains the fix, float solutions and blunders in control point 2. The blunders are picked out by the largest w-test value in one direction, which means even if one measurement behaves good in two directions, it can still be detected by the very bad performance in another direction. Not only fix solutions are reliable, but also a large amount of float solutions is of good quality.

Although the measurements are taken continuously, there is still large difference in measurements quality between sessions, among them, session 1 and 3 have relatively more reliable measurements. During the experiment, the available satellite numbers are around 5 or 6 but still acceptable, this may be owing to the location of control point 2. Although it is surrounded by farms, there is a wind mill by 10 meters away, so the available satellite numbers may be reduced by this obstacle. With less satellite numbers, session 1 and 3 still get comparably better measurements, this might due to a relatively better satellite geometry. To have better quality of measurements, the location of control point should be selected carefully, with no obvious obstacle too close.

What's more, the covariance is computed only by fix solutions in this case, the number of them can be improved by using more flexible constraint, e.g. covariance from float and all measurements accordingly. Here is an example on using larger covariance in w-test, from Fig. 5, as one can expect the outliers are less than using only fix solutions, which can better represent the data performance, more applicable especially for one control point has more float measurements.

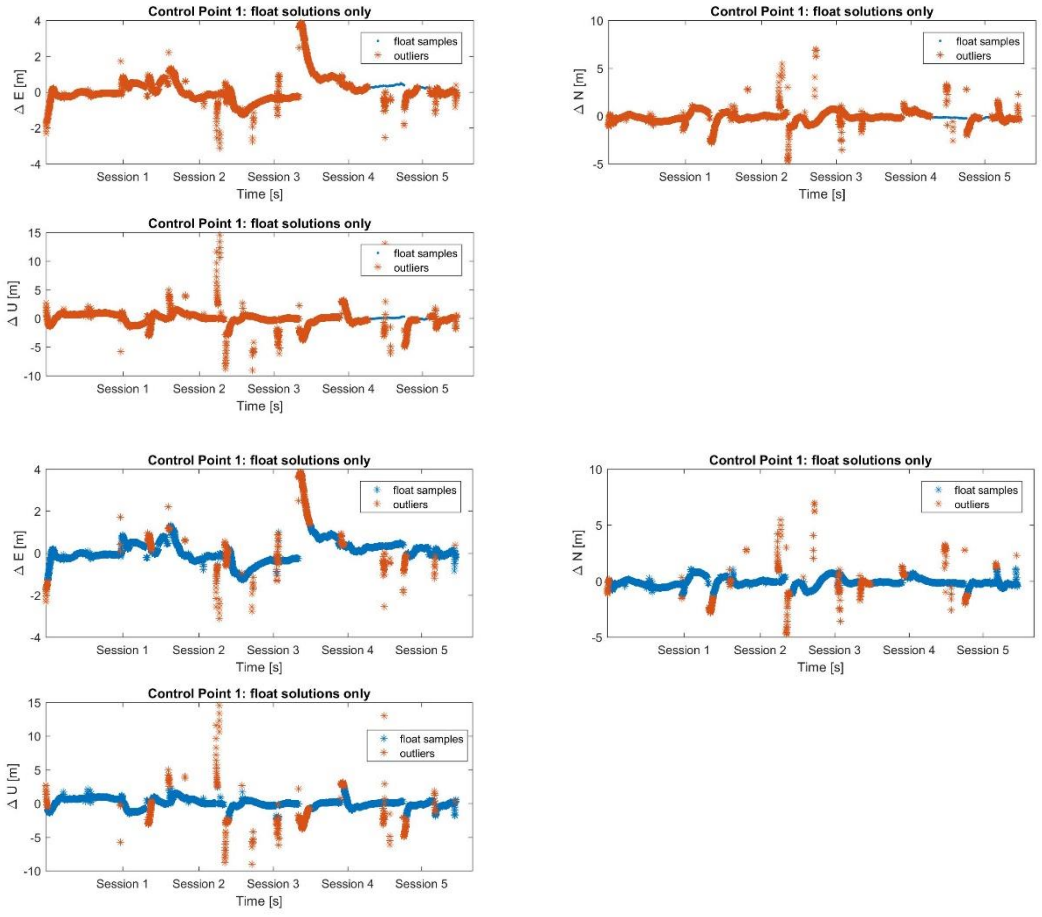

Figure 5. Time series of control point 1 float solutions: the upper results are by using covariance computed by fix solutions, lower one is by covariance from float solutions.

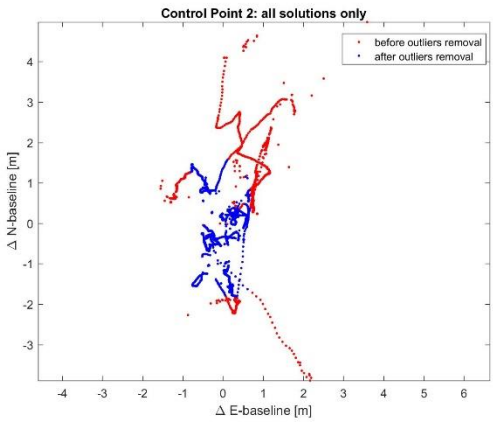

Figure 6. Scatter plot of measurements before and after outliers removal in North and East directions.

The scatter plot shows the measurements in the North and East direction. The measurements are more concentrated in East direction than the North, which means it has smaller standard deviation in this direction.

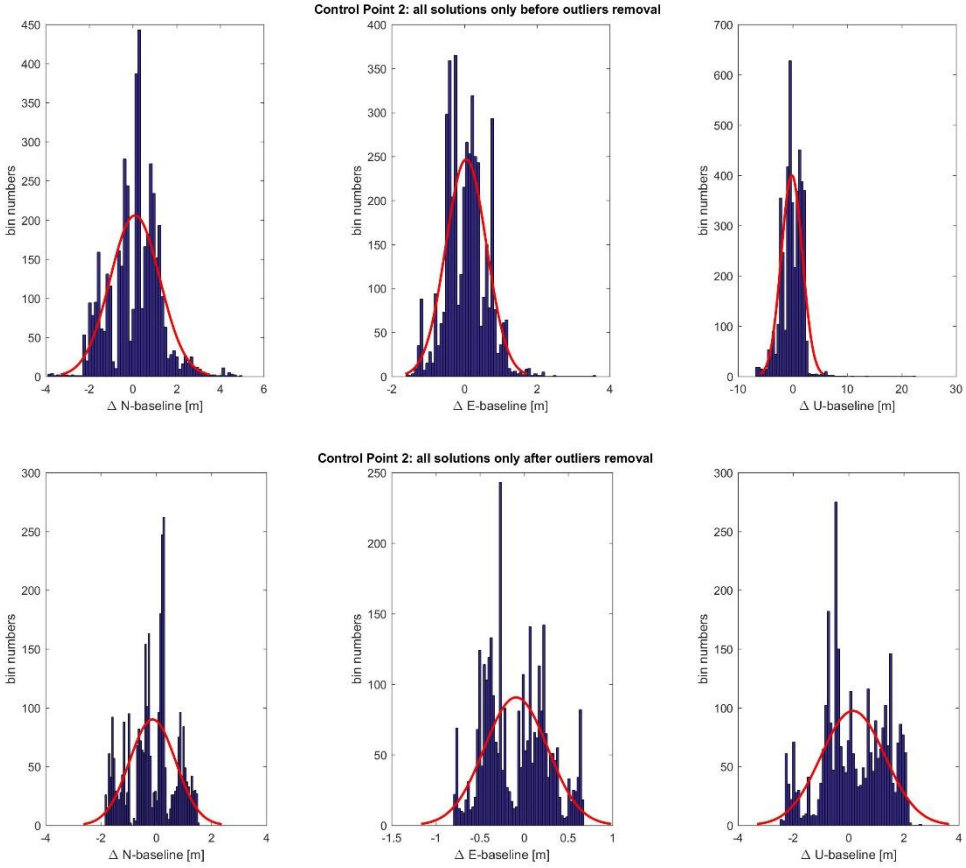

Figure 7. Histogram of all solutions in control point 2 before and after outlier's removal.

Figure 7 shows the distribution of measurements before and after outlier detection procedure. Before removing outliers, the dataset has zero mean in three directions, the North and

East direction have nearly normal distribution, while in Up direction is hard to see and it has very large range due to some very bad measurements. After removing outliers, the range of Up direction is improved.

After obtaining the separate results for each control point, then we compile them with the baseline length, TTSF, fix percentage, outlier ratio and environment information to further exploit these factors' impact on measurement performance.

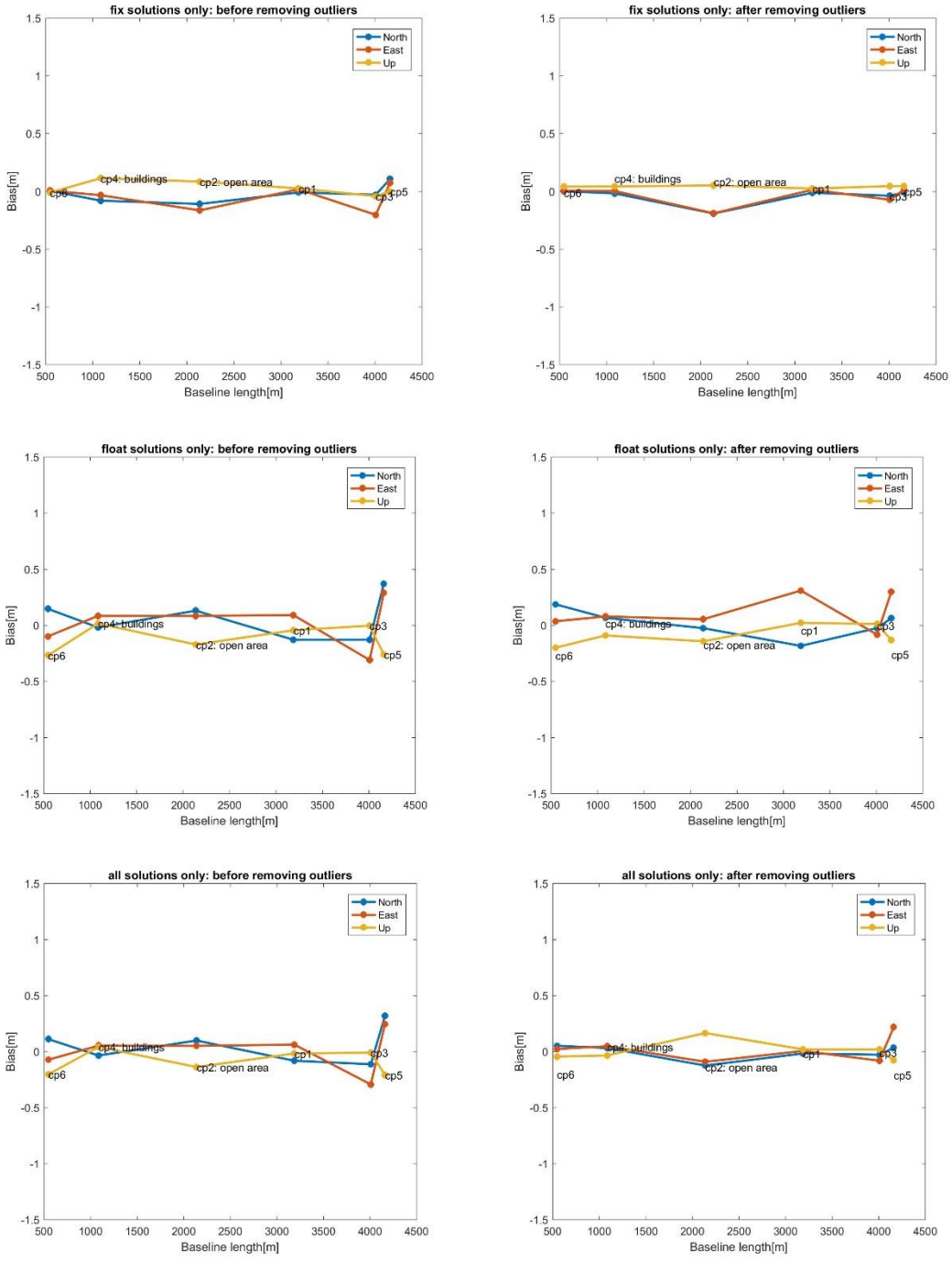

Figure 8. Bias plot of fix, float and all solutions of all control points vary with baseline.

We can see from the Figure 8 that fix solutions have better accuracy except for the control point 5, then follows when all the measurements combined. And this large bias is resulted from really bad performance especially from last three sessions, there are several measurements with more than 100 meters far off from the ground truth solution, owing to the less available satellite number with good signal. The possible reasons are the changing multipath effect of signal and comparably less available satellite number in last three sessions. The outlier's detection procedure improves the accuracy in three cases and improves more when combing all the measurements. While for the float solutions in control point 2, the procedure seems like not working properly due to the enlarged bias, this is because in the model, we use the mean value as the optimal estimation to reduce the computation power. The larger bias after w-test means the mean of the float measurements is far off from the truth. This can be improved by using the mean value of the fix solutions. The influence of baseline length has on accuracy is not obvious and hard to evaluate, for example control point 5, the curve is greatly influenced by several bad measurements, and we couldn't decide which factor contribute to this, the result can be improved by taking more sessions of measurements, and take records of the environment, sky plot, elevation angle and log base station data, during and after the experiment respectively.

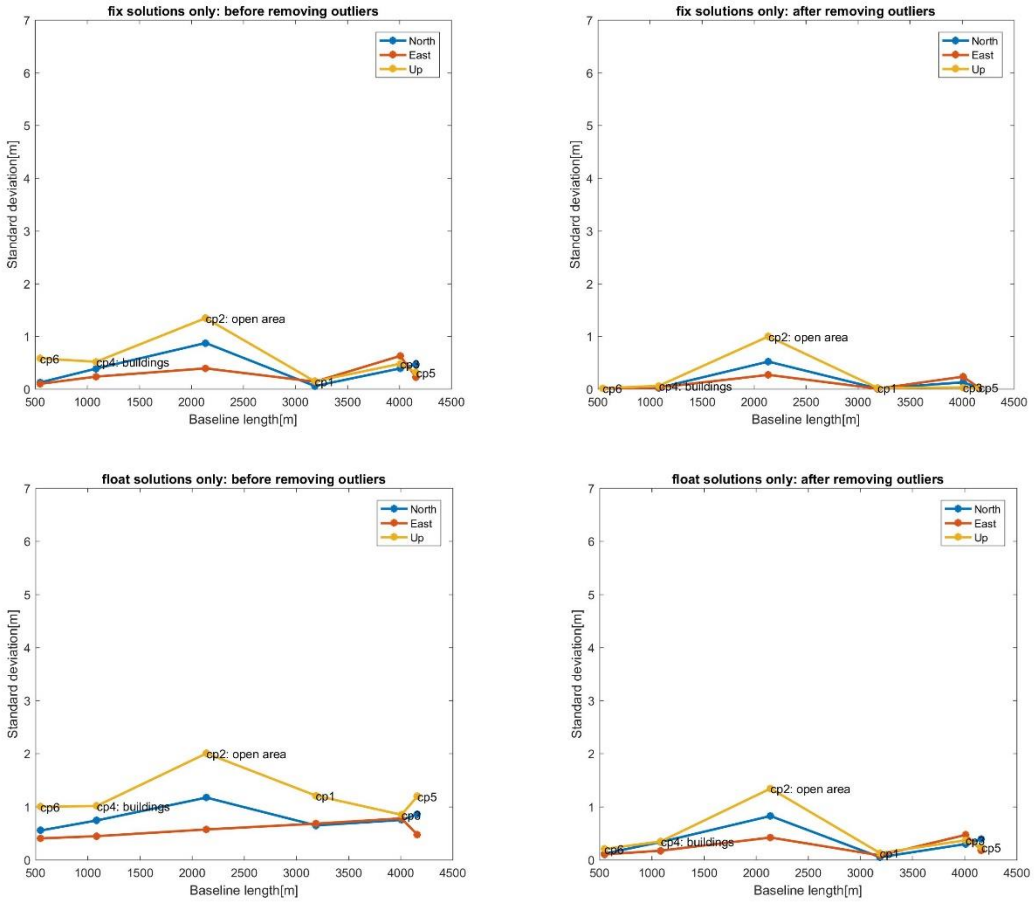

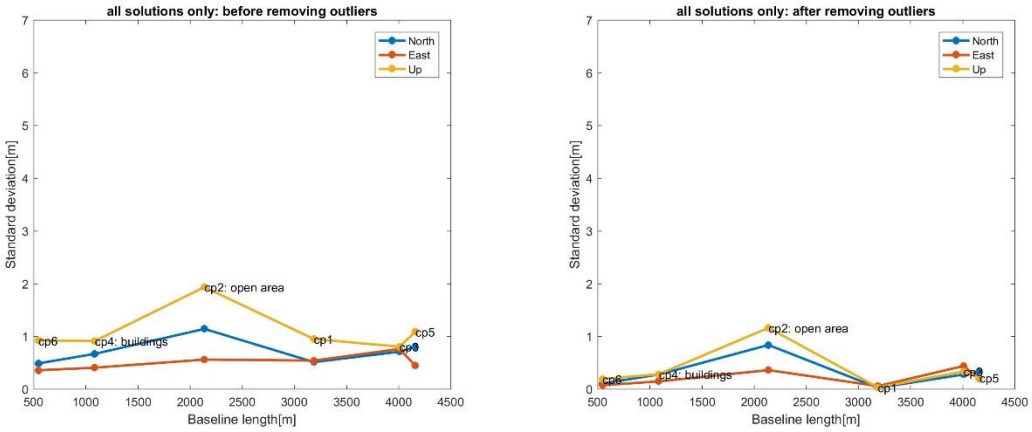

Figure 9. Standard deviation plot of fix, float and all solutions of all control points vary with baseline.

From Figure 9, control point 2 has the worst precision especially in Up and North direction, the reason probably is the less satellite number in the view and the multipath effect, although it locates on farms, there is a wind mill nearby. Also the Up directions especially on the left three plots have less precision, and on the right three plots, the precision improved because the procedure picks out most influential measurements, and in this case, many of them are in of the Up direction. The outlier removal procedure improves the precision in all three cases, and the precision of all measurements is even more reliable than the fix solutions before the procedure. The precision variation along with baseline still not obvious, we couldn't decide which factor contributes to the really bad performance, and the trend along with baseline length is not obvious either. For the really bad performance in control point 2, removing session with bad measurements according to the time series will indeed improve the statistics in all three plots. On one hand, it is hard to have the standards on how many sessions to remove, and whether it is applicable to other control points. On the other hand, even the standards are reasonable and the statistics are improved after, it is still hard to draw the conclusions on influence of baseline length.

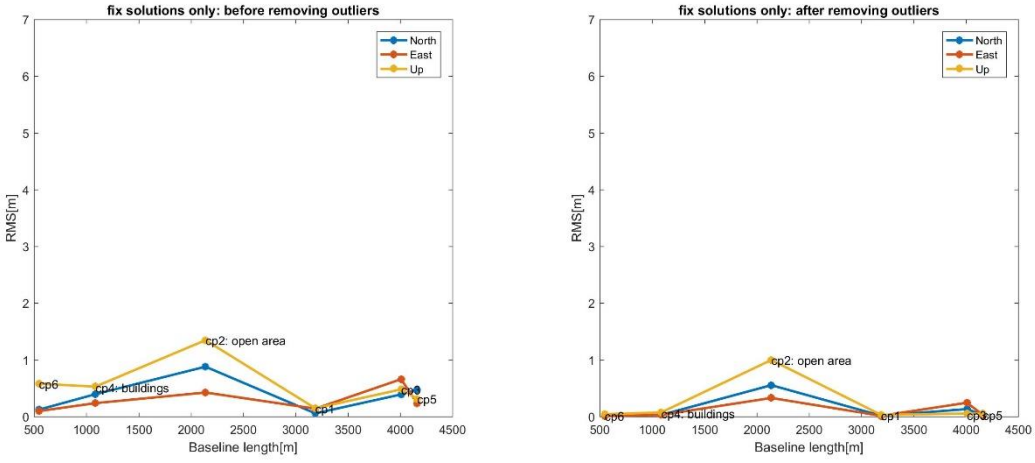

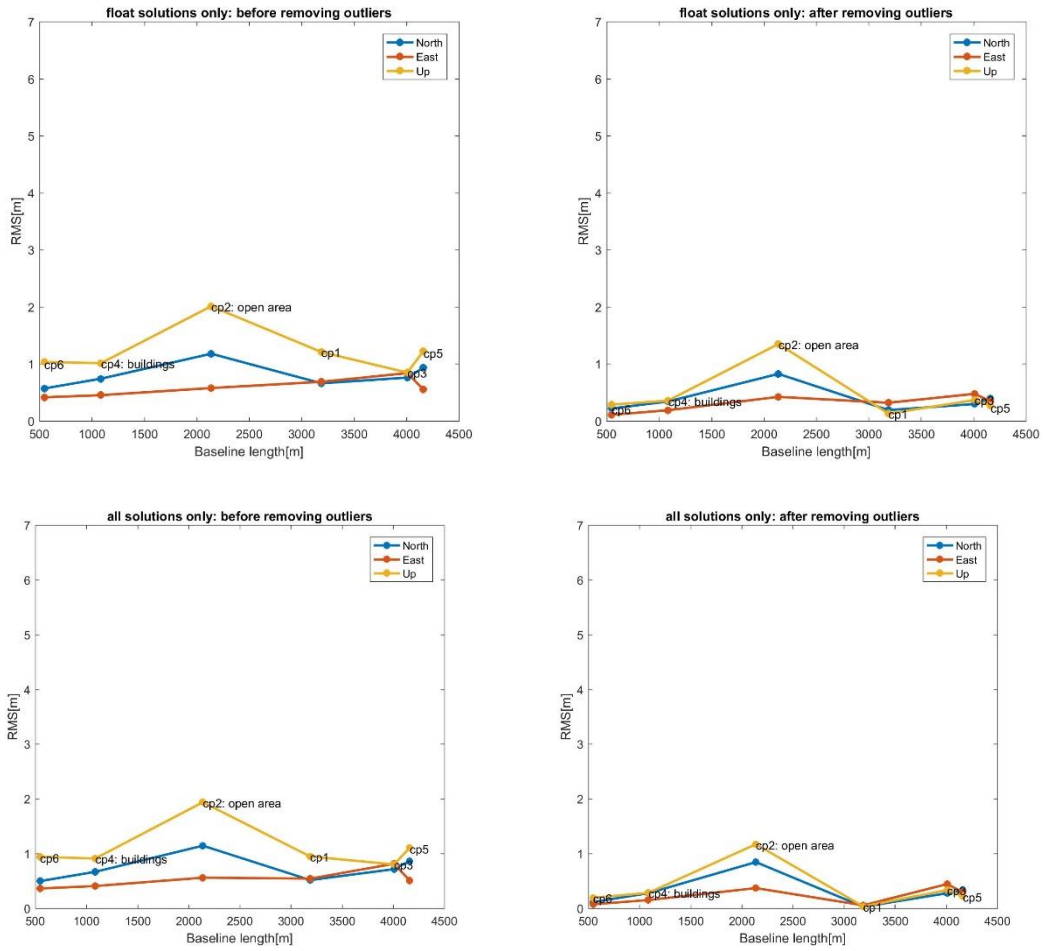

Figure 10. RMS plot of fix, float and all solutions of all control points vary with baseline.

Figure 10 shows the RMS changes before and after the procedure. Control point 2 has the worst RMS especially in Up direction, this is mainly resulted from poor precision. Control point 5 has less accuracy but good precision, so the performance of control point 5 is not bad even though with the longest baseline length. This is because the standard deviation contributes the RMS more because it has larger value than bias, so RMS performance heavily depends on their precision performance. Also the Up direction is less trustworthy than other directions especially before removing outliers. This probably because of the high VDOP which on low horizon will result in poor vertical measurements. To improve this, one can take down the elevation angle while experimenting, and try to avoid a lower one. Comparing the figures on the left with on the right, we can see that after removing outliers, the RMS values are improved in all control points except for the second one, due to the large precision after the procedure. Therefore, there is no obvious trend of RMS varies with baseline length.

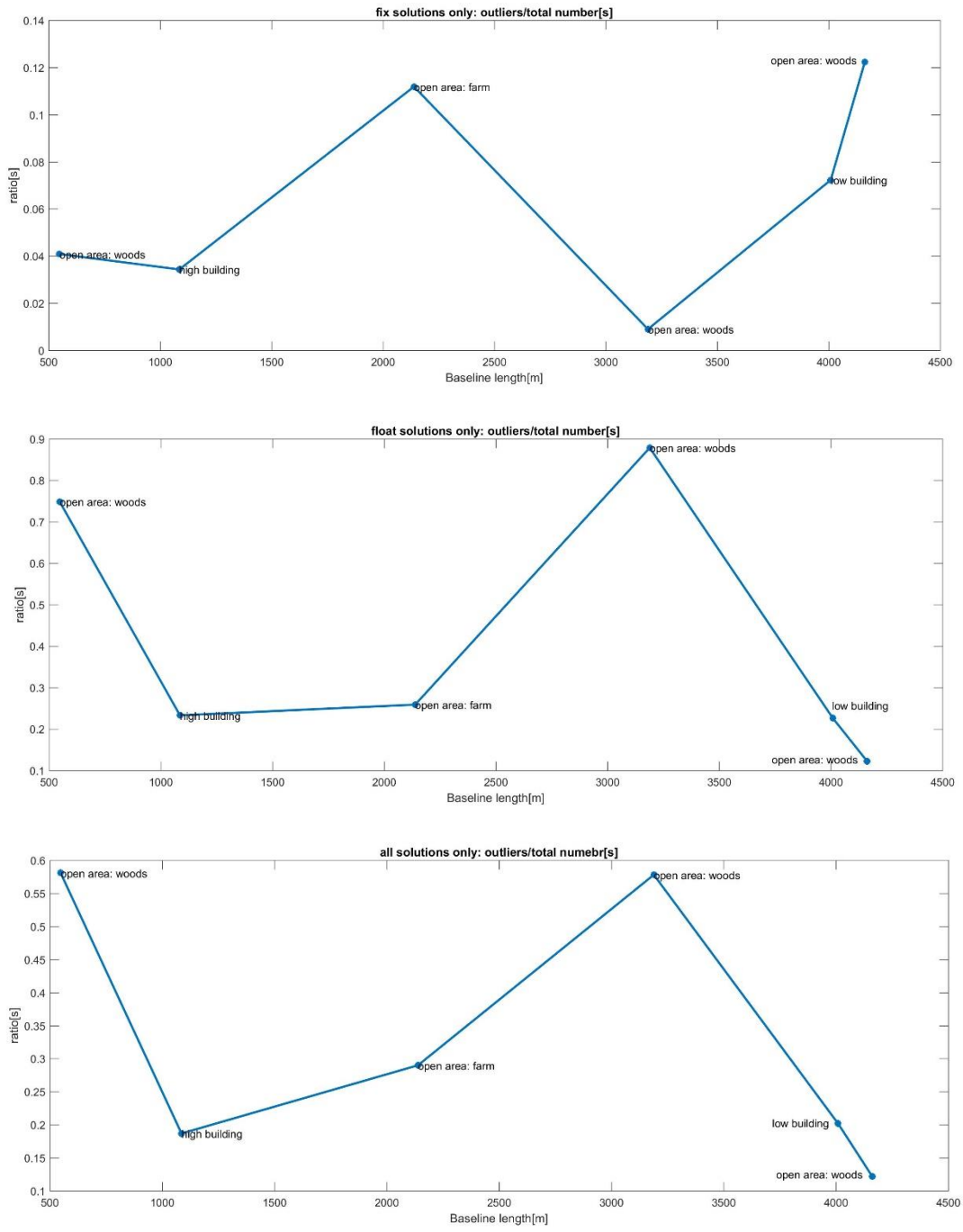

Figure 11. Outliers ratio plot of fix, float and all solutions of all control points vary with baseline.

Figure 11 above shows the ratio of outliers by the input samples. For fix solutions, the ratio = outliers number in fix solutions / fix solutions number. The smaller the ratio is, the more reliable input samples are. We can see that fix solutions have less than 12% of removing rate, and has opposite trend compare with the float solutions and all measurements combined. The bellowing two figures have almost the same trend, which means the outliers are determined by the quality of float measurements.

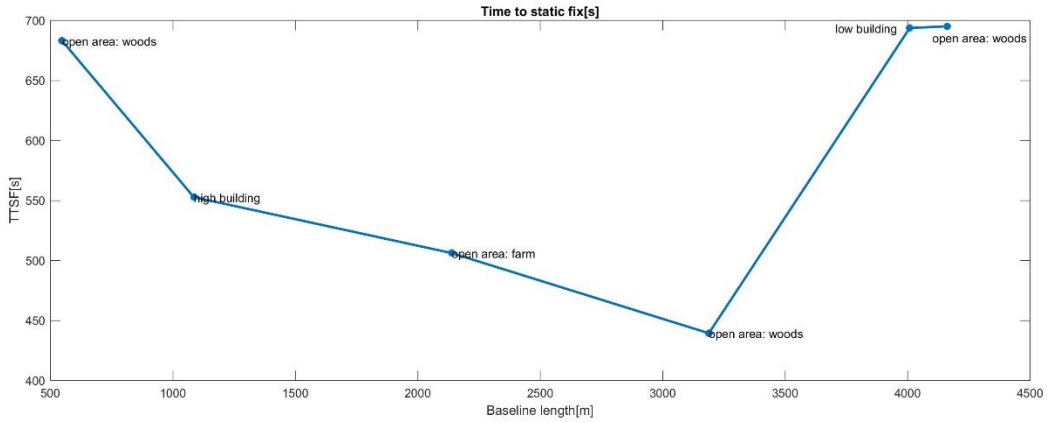

Figure 12. Time to static fix of all control points vary with baseline.

Above Figure 12 shows the TTSF varies with baseline length. We first determine the start time of more than 100 fix solutions in one session, and then take the average of all found start time in one control point. We can see that the range of TTSF varies from 6 min to 11 min, decreasing greatly with baseline length in first 3200 meters and then increase sharply. Along with Figure 10, although we add some surrounding information of the control points, it is difficult to tell the trend and determine how much the topographic influence have on the measurements.

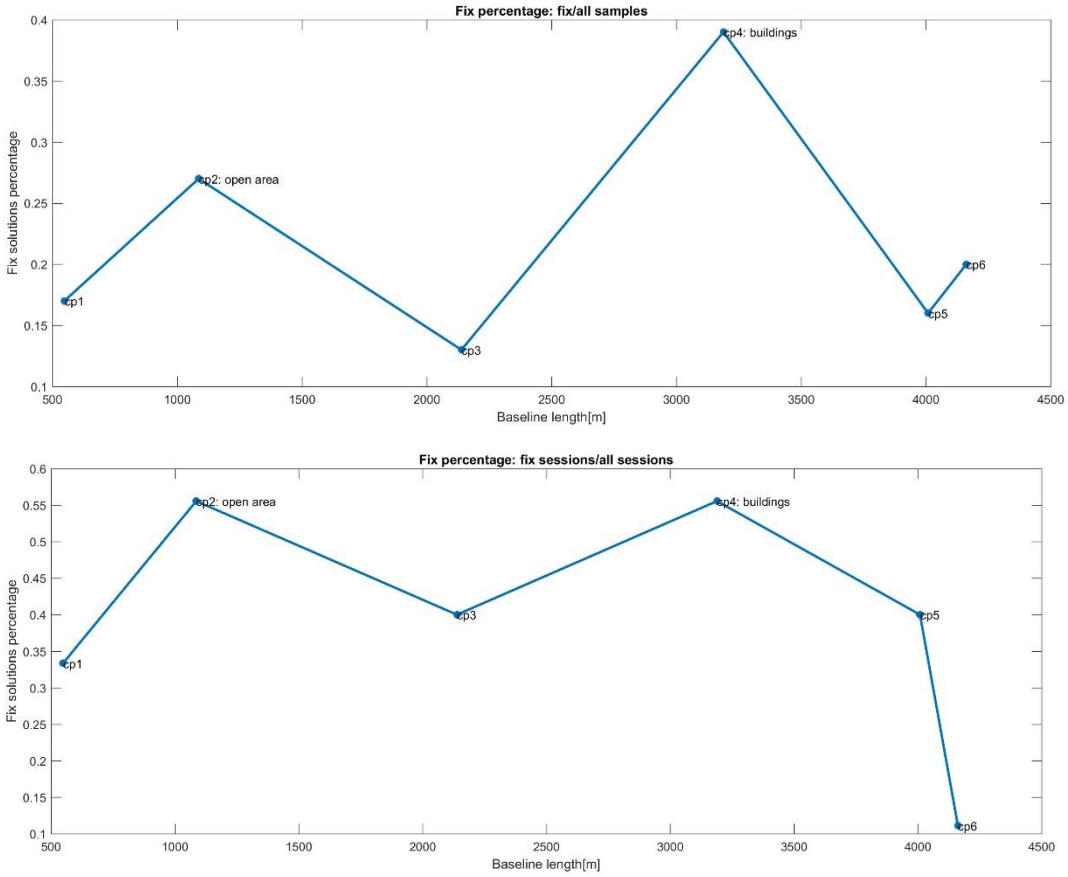

Figure 13. Fix percentage by sample numbers (top) and fix percentage by sessions (bottom) of all control points vary with baseline.

Figure 13 shows the fix percentage by computing sample ratio and session ratio respectively. We can see the trend of the two figures are quite similar, except for control point 6. This means that the more sessions have static fix solutions, the more fix solutions we will have. For control point 6, there is only one session have static fix solutions, and there are a lot of random fix solutions in the rest of measurements.

Conclusion and discussion

For the experiment, we define the 'time to static fix' as the start time of at 100 continuous fix solutions in one session, which is selected by quality flag = 1 in the solutions file. The assumption also works for when determining the covariance matrix, where we select the fix solutions in one control point, although they probably have different fixed ambiguity, instead of using the standard deviation in the solutions file because it is too optimistic. The smaller covariance values will lead to less tolerance in the outlier's removal, therefore, few solutions can pass.

The model RTKLIB is used to process the observations assume that the observations errors conform the standard normal distribution. And in the outlier's removal step, we also assume that by computing normalized residual, the observations conform the normal distribution with the zero mean. Before outlier's removal, the histogram of measurements is off the normal distribution because of the bad measurements as well as the RTKLIB model error; the histogram after the outlier's removal is off is due to the assumption in the outlier's removal, the step can be improved by using constraint of the 95% confidence interval of measurements.

Although by introducing the simplifications, the computation time is greatly improved, this method may result in smaller w-test values, which means the number of measurement that are below the critical constraint is larger. So in reality, the number of outliers is larger than what we have now. As the iteration goes one, the dimension of the covariance matrix is decreasing, so how much does this smaller w-test values that comes from the simplifications will have on the final solutions is still uncertain.

From the time series plots and summary plots of statistics, we can see the outlier's removal procedure is working, most of the unreliable measurements from East, North or Up directions are removed; and the precision and bias is also improved. The more outliers in the fix measurements, less concentrate the fix dataset will be, which means the covariance matrix has comparably larger value, which will allow more float solutions pass. While when combining all measurements, the majority of the data is of float flag, and we compute the mean of the dataset as the estimation, which means the estimation will incline to the float measurements' mean, and at the meantime, loose constraint allows more float solutions pass, which will add the weight of float measurements in all measurements performance, thus, the two lines, outliers ratio of float and all measurements show the same trend, and the fix measurements' curve shows the opposite trend.

From the bias and std plots, we can see for control 2, the measurements are of poor quality. The large bias is owing to the difference of the estimation of selected data used in w-test model and the ground truth coordinates. The bad precision is caused by large number of bad measurements in data. Bad satellite geometry and less satellite numbers are the possible reasons. However, the outlier's ratio plot indicates that there less outliers removed from these two control point, which means many unreliable measurements pass the w-test. This can be resulted from larger value in covariance matrix, which gives a rather loose constraint in computing w-test values. Since we

derived the covariance from fix solutions in one control point, that means in these control points, the fix solutions are not reliable either, especially for the float measurements. For example, control point1 float measurement time series, the covariance matrix is too strict in this case, and few float measurements are usable. In this case, the covariance matrix can be computed by float measurements within certain time interval, and update for float measurements in next time interval.

From the RMS plot, we can see it has almost the same trend and values as the std plot, which means in our case, RMS depends on std since the std values are much larger than the bias. The quality of data can be influenced by many factors like radio interference, multipath effect and ionospheric delay, so it is hard to differentiate those factors' influence with the topographic and baseline length effect. At the meantime, for easier implementation of the experiment and time limitation, the selection of control points are not sufficient enough to evaluate the baseline length and topographic influence on measurements. To improve this, following experiment can be conducted on more control point with same baseline but with different surroundings, and with more information taken down, so we can have more contrast internally.

TTSF is based on the average value of TTSF in a control point. Control point 5 has only one TTSF, control point 2 and 3 have two TTSFs, so the values are unreliable since there is less sessions have static fix solutions. The fix percentage rate computed by sample ratio and session ratio have very similar trend except for control point 6. This is because the sessions have static fix solutions are less. The reason might be improperly defined TTSF, 100 may be strict especially for control point 6.

Part II:

In previous experiment, the ground truth coordinates for each control point and base station are already known precisely, therefore, by constructing the local reference system with its origin on base station, rover position can be easily referenced under this local CRS. However, in reality, it is rare to see that a surveyed reference station is suitable and available for one's implementation. What's more, the base station coordinates accuracy will also contribute to the RTK accuracy, an error of 10 in base station coordinates leads to one part per million error in the baseline vector (Trimble.Inc, n.d.). In this case, especially for the construction of a dense low-cost base station network, coordinates for the newly constructed base stations need to be determined with good precision. So in this part, we will introduce four approaches can be used to acquire base station coordinates.

NETPOS product

One common and convenient way to determine base station coordinates is to use NETPOS GNSS products. The services provide GPS and real-time corrections for positioning in ETRS89, and have corrections for the observations from its product with high accuracy.

NETPOS (Netherlands Positioning Services) consists of Netherlands permanent GNSS-Infrastructure hosted by *Kadaster*, *Rijkswaterstaat* and TU Delft to have high performance in

positioning. The network is designed to link all reference stations to a central data processing center to obtain optimal calculations, and then provide real-time, highly reliable positioning services to the rovers (Qu, 2012). The system makes use of 34 of the 40 reference stations with a spatial interval of 40 km, and provides real-time services and post-processing services, which enables users to make measurements everywhere around the whole country. With the in-company data communication networks in transmitting and receiving signals from the reference stations and GPS and GLONASS, therefore, an improved cm level accuracy with high reliability is guaranteed.

Approaches:

Real-time approach:

To create a new base station, if the receiver is Internet-connected, a first approximate position will be made once connecting to the NETPOS network with the receiver by, e.g. a mobile phone. A Virtual Reference Station (VRS) is selected according to this approximate position of the new unknown base station by NETPOS. Then the NETPOS will send this user VRS data (correction) to the under-determined base station location.

When the rover receiver has Internet connection, the input NETPOS VRS data from rover receiver (locates on the unknown base station) e.g. Ublox, and correction from real-time products can be combined in real-time by RTKNAVI on a Windows PC or RTKGPS+ on an Android phone, then the exact observations for the unknown position will be determined, user can save the observations from the output option.

Post-processing approach: NETPOS product

However, in case some of the receiver has no access to internet, post-processing procedure can be helpful. SSRPOST is to retrieve accurate positions by processing GPS carrier-phase data, and state vector (corrections) is produced by the service. RINEX file from the unknown base station is needed to upload, which can be obtained by RTKCONV to convert the raw observation data, and the position measurements are in ETRS and its quality will be returned.

Post-processing approach: RTKPOST

Another post-processing procedure is by using RTKPOST. Users can have their specific settings according to different needs. A RINEX file of the observation and corrections from a known reference station by NETPOS are uploaded, then users change the options by RTKPOST processing, and run the execution window. The final solutions will be returned according to users' preferred format.

Post-processing approach: Bernese Software with selected IGS/EPN

Another post-processing method for unknown base station position determination is by using the International GNSS Service (IGS) and EPN (EUREF Permanent GNSS Network), RINEX observation files and the Bernese GPS software. IGS provides high-quality GNSS data products with more than 400 reference stations worldwide (IGS, 2017). EPN conforms the same consistency with the IGS standards so as to make densification in European countries (Drewes, 2009). Until now, there are 6 EPN/IGS in Netherlands and several surrounded candidate ones around the country depends on the location of the unknown base station. Most of these stations can provide daily/hourly/real-time data. When select the possible IGS/EPN sites (fiducial sites) around

the base station to be known, one should be aware: 1) the more is better 2) distance should be within 1000 km 3) the sites has defined ITRF coordinates and recent data are available and steady (Douša, Filler, Kostelecký, Kostelecký, & Šimek, 2010). Then input the RINEX observation files and select the IGS/EPN station to include, processing can be done by Bernese Processing Engine.

Summary

In this part, we have discussed four common approaches to determine an unknown base station. Three approaches need corrections from NETPOS except for the last approach. In first two approaches, users have no influence in processing, after uploading the observation RINEX file, the final solutions will be returned. While in the last two approaches, user can have their own settings by using RTKPOST or Burnese, they can use specific configuration to do the processing. What's more, the software Burnese and the selected IGS/EPN are open source, so it is free for user to apply this approach. The precision from first two approaches is guaranteed since NETPOS provide the final solutions, the last two have more uncertainties because the users have more choices.

However, for a low-cost base station construction, user may need to try several locations before it get stable measurements. Since the low-cost base station is easy to setup, it is much easier to change to another site once user find the measurements are not good. As soon as the measurements are good enough, one can use one of the approaches to determine the unknown base station position.

Table 1. Summary of differences between four approaches.

	Input entry	User influence	Area limitation
Real-time NETPOS	Virtual RINEX	No	Within NETPOS coverage
Post-processing NETPOS	RINEX	No	Within NETPOS coverage
Post-processing RTKPOST	RINEX RTKPOST	Yes	Within NETPOS coverage
Post-processing IGS/EPN	RINEX Burnese	Yes	Depends on available IGS/EPN sites

Part III:

This part gives you a detail introduction of whole experiment setup, including the needed hardware, connections with them, and configuration with the software. Users wish to apply the same application can conform the following steps.

Hardware preparation

The experiment deployment is based on NETPOS One concept, which is a precise positioning technique based on single frequency RTK reference network. Its goal is to convey a more convenient and cheap way to have precise position measurements. Users can obtain positions via the rover setup (mobile phone with RTKGPS+ app installed) by getting access to NTrip caster, which can record, transfer and process the data from base station and send the corrections to the rover (mobile phone). Cheap price, convenience (portable rover setup) and accurate solutions make it competitive and have massive market.

Base station section: satellite signals are received by antenna connecting to the receiver (UBLOX EVK-M8T) of base station, connect computer/Raspberry Pi by cable (micro-USB-USB) and process there with RTKLIB (STR2STR). The data then be transferred to NTrip caster with internet connection to provide corrections for the RTK operation.

Rover section: signals are received by antenna connecting to the UBLOX EVK-M8T, then connect the receiver with smartphone/Windows PC by cable (micro-USB-USB) and OTG/ cable (micro-USB-USB), and at the mean time have access to NTrip caster (Internet) to retrieve corrections. Then the raw data from rover receiver and corrections are processed by smartphone with RTKGPS+/computer with RTKNAVI to obtain the rover's position.

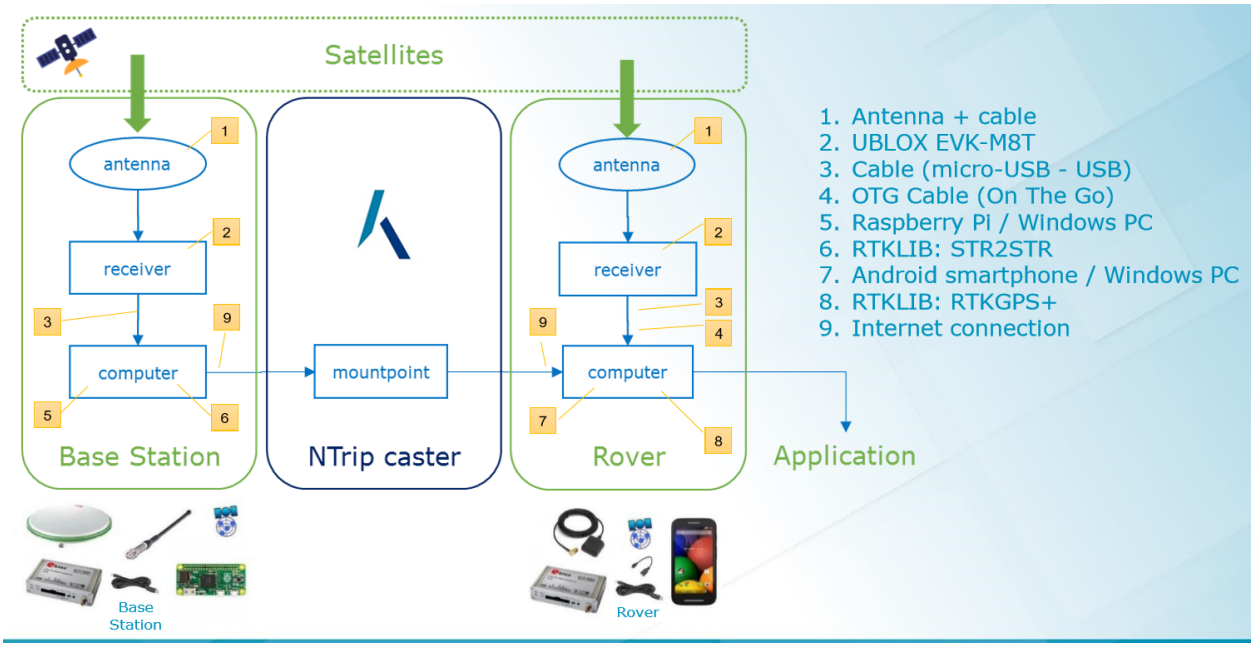

Figure 14. Netpos One conception map.

UBLOX EVK-M8T: data have been collected by this receiver, used in both base station and rover setup, connect to antenna and Windows PC/Raspberry Pi (Base station) or Windows PC/smartphone (rover)

Antenna + cable: used to connect with UBLOX EVK-M8T in both base station and rover setup, different types of antenna have different performances.

Android smartphone/Windows PC: in rover setup, an Android with app RTKGPS+ can act as Windows PC with installation of RTKLIB v2.4.2., because the observations from both kinds of devices are actually processed by RTKNAVI, and they are connected to the UBLOX EVK-M8T. Need Internet connection to retrieve data from NTrip caster. And the rover position can show up on RTKGPS+ and Windows PC RTKNAVI interface.

Raspberry PI/Windows PC: in base station setup, use to process base station data and transfer it to NTrip caster, connect to the UBLOX EVK-M8T. Internet is needed to transfer/log data to NTrip caster.

Connections: OTG cable + Cable(micro-USB-USB) for connecting smartphone and UBLOX EVK-M8T; OTG cable only for connecting UBLOX EVK-M8T with Windows PC/Raspberry Pi.

Software configuration(format)

STRSVR is used in base station setup in order to divide the input stream into multiple streams, then pass the output streams. Detail configuration for the input/output streams are shown in following figure. And access to a mountpoint and password is needed.

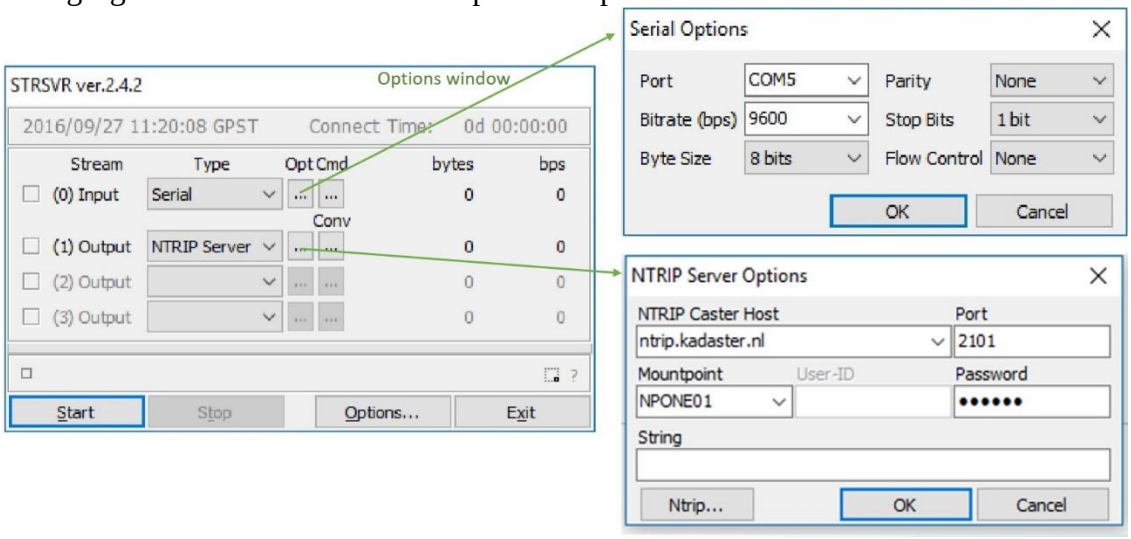

Figure 15. Settings for STRSVR input and output stream.

Then click the start button, if the application goes well, the light should turn green; if one wants to stop it, type Ctrl-C in the console.

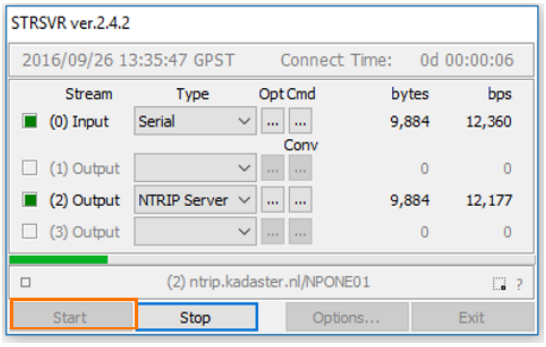

Figure 16. STRSVR ongoing operation window.

Application RTKNAVI in rover setup is to process data in real-time. It requires the raw observation from rover and corrections receiving from NTrip caster. User can select the display

switch on the left to change coordinates format; the right ones can show different monitoring screen, and one of them present the rover and base SNR (signal to noise ration), which can be used to check the signal quality. Here is an illustration map of main icons on RTKNAVI display screen.

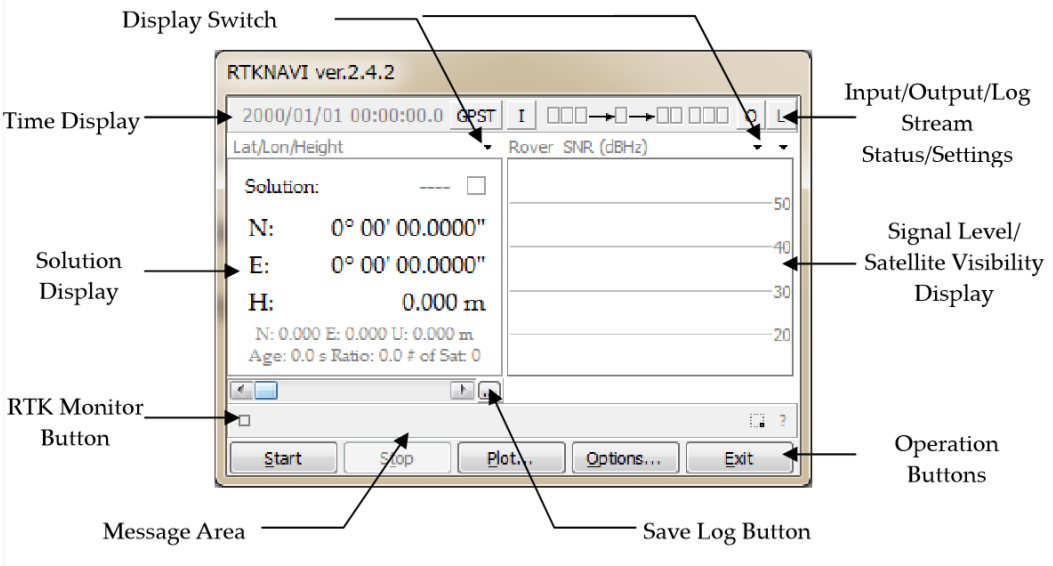

Figure 17. RTKNAVI main execution window (Takasu & Yasuda, 2013)

Here is the configuration for input stream.

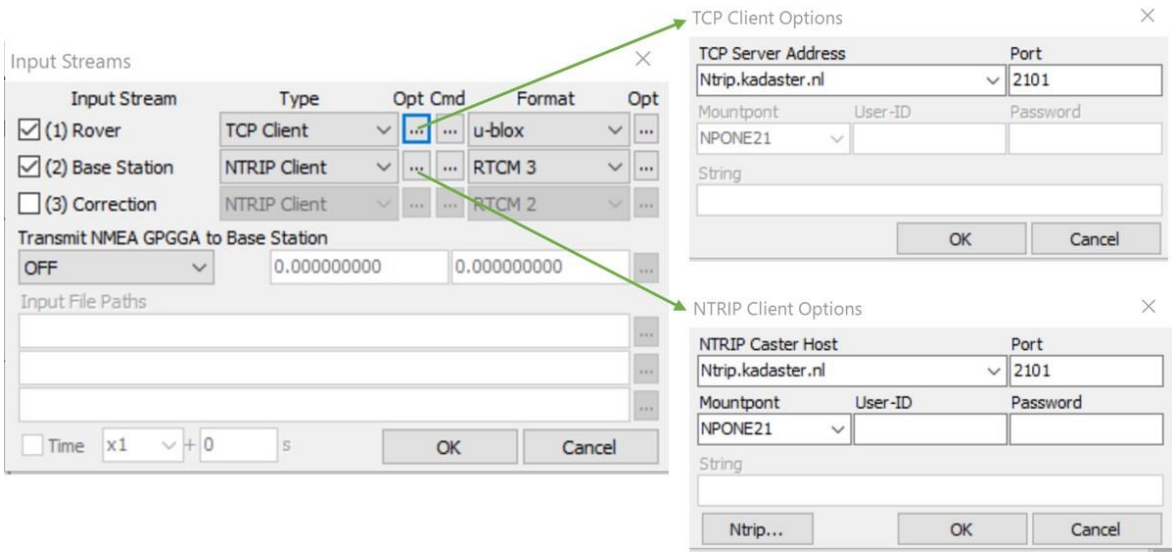

Figure 18. Settings for RTKNAVI input and output stream.

After setting up the input stream, one can save the file in different format and change the path. And the 'file' format usually can be opened in txt. Then the application is ready to run. The following figure shows an example of operating in state. In SNR plots, only dark green means connected or running, light-green means data active, others indicate the errors or improper connection. User can check the scatter plots of measurements by clicking 'Plot'.

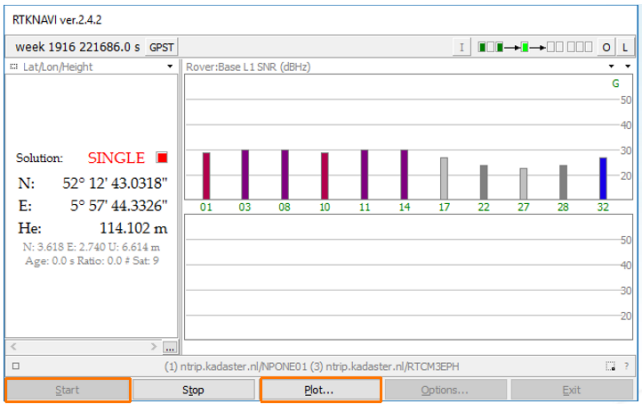

Figure 19. RTKNAVI operation window. Green light by the side of input stream indicates the software works properly.

In the base station and rover setup, UBLOX EVK-M8T are used as receivers, and several steps are needed before the application.

First, users need to download the u-center for Windows users (https://www.u-blox.com/en/product/u-center-windows). Go to main menu l 'Receiver' >-'Generation' , user can select their own type of UBLOX, here we use type EVK-M8T as an example.

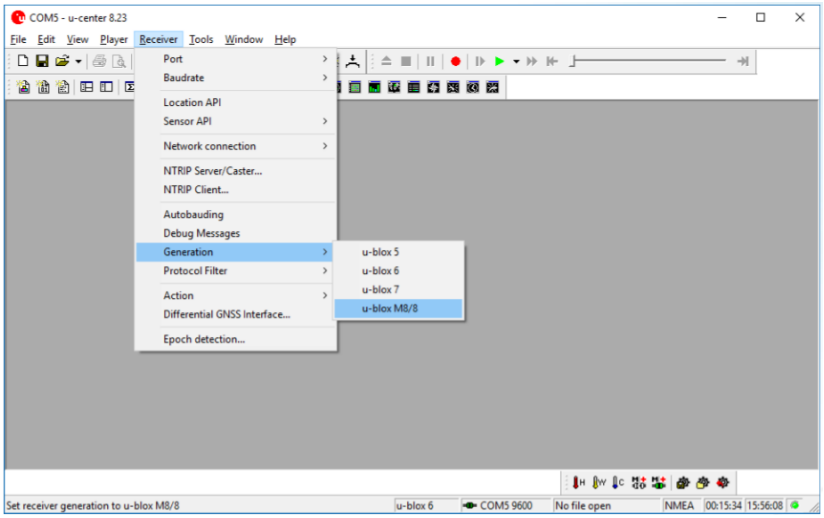

Figure 20. Main execution window of U-center.

Connect the receiver with the USB cable to the computer, then locate to the communication toolbar and click 'connect' button and choose 'COM5' to create a link with the appropriate COM port. User can select the baud rate of the receiver (typically 9'600 baud). If the connection is good, the icon will turn green, and this means the u-center operates properly. It's ready for one to use the receiver.

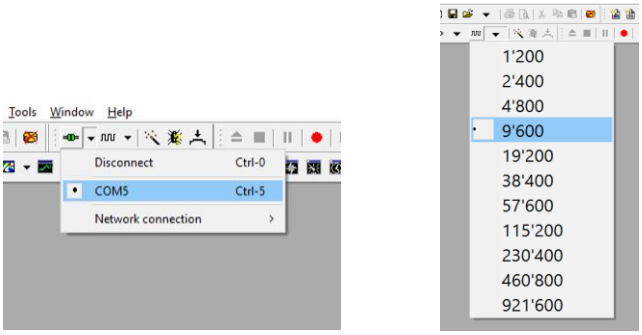

Figure 21. Zoon in icons of communication tool bar.

Select 'View' >-'Configuration View' and then choose 'PRT(Ports)' on the left column which gives you the following window. This option display message to configure the receiver (Ublox, 2016). 'Select '3-USB' under 'Target', '0+1 UBX+NMEA' under 'Protocol in' and 'Protocol out' respectively. And click 'send' on the bottom left.

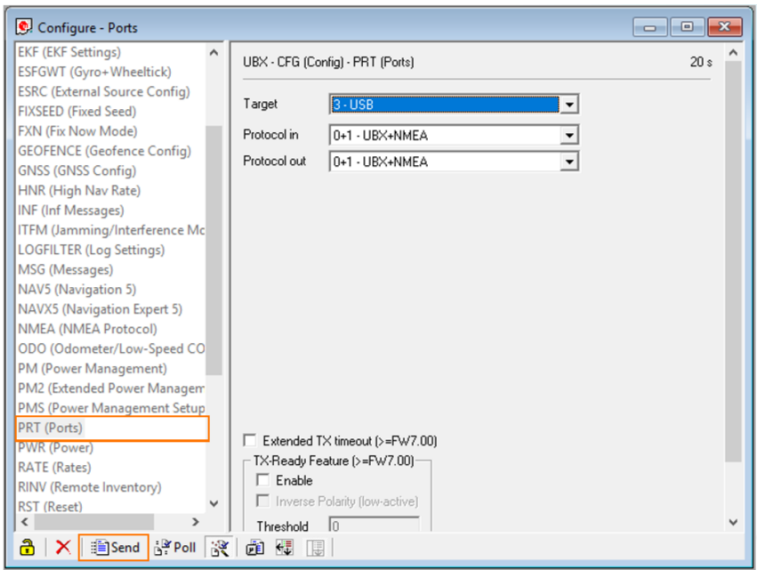

Figure 22. Detail setting for 'PRT(ports)'.

Then go to the item 'GNSS (GNSS config)' on the left columns and change the setting: select all configures, and enable GPS, Galileo and Beidou. Then fill in the 'min' column with (8,1,5,3,0,0,8), and 'max' column with (16,3,8,8,8,3,14), and cross all the signals options. And click 'send'.

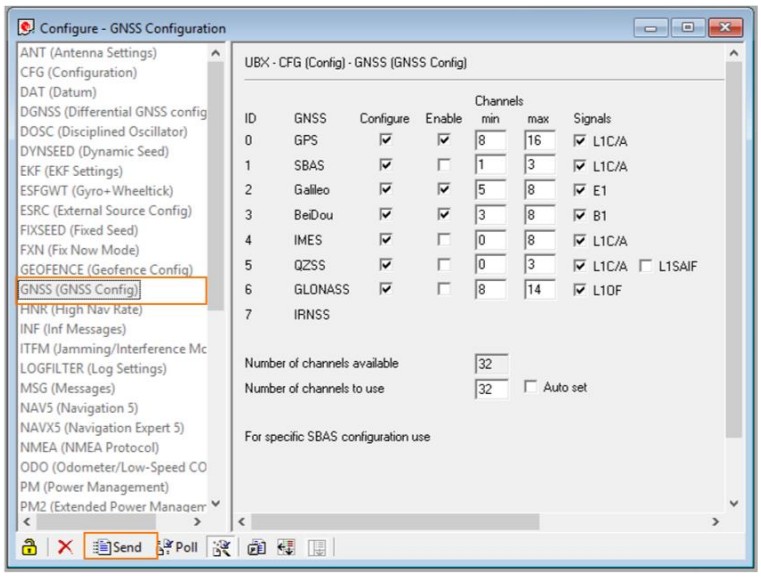

Figure 23. An example of GNSS (GNSS Config) setting.

Choose ‘MSG(messages)’ from the left column, draw the ‘Message’ list and select ’02-15 RXM-RAWX’. Then enable USB and set the value as ‘1’. And click ‘send’.

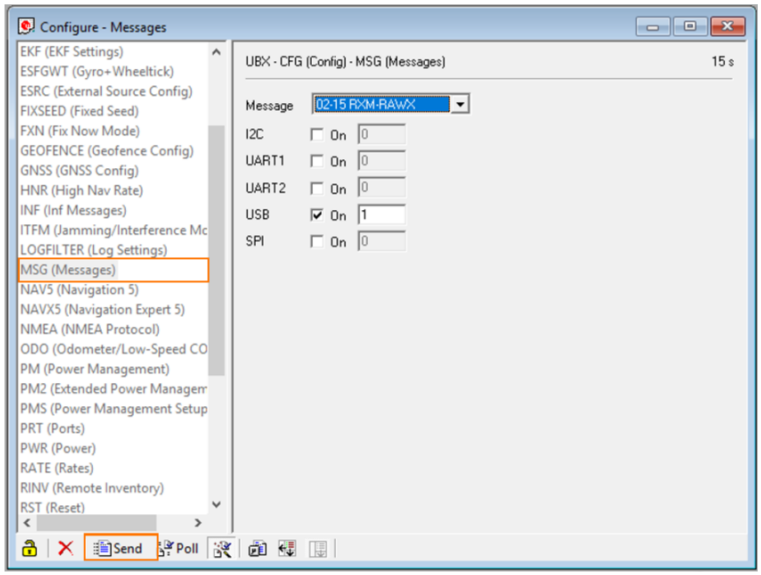

Figure 24. Options for MSG (Messages).

Go to the left columns again and choose ‘CFG(configuration)’ this time, cross ‘Save current configuration’, and click ‘send’. Now the settings are saved in Flash.

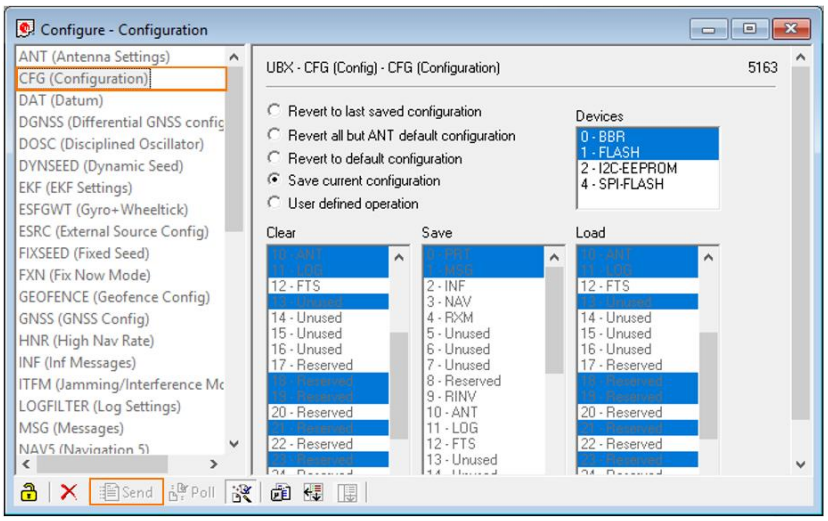

Figure 25. Saving the configuration of current changes by CFG (Configuration).

Now the receiver M8T is ready to use, user can go back to the main console and run the application.

Conclusions

The outliers' removal procedure in processing the measurements in the experiment indeed improve the solutions performance. Based on our simplified outliers' removal model, we find the quality of float solutions determines the performance of all measurements in one control point, and the number of sessions that have static fix solutions can be critical to get fix solutions. The obstacles, baseline length influence on measurements performance are still uncertain, due to the simple deployment of limited control points in the experiment and insufficient record.

Further experiment can be conducted on two groups: more control points of with more similar environment; more control points with the same baseline but larger variation with their surroundings, and taking more sessions of measurements due to the instability in control points' time series. And in both scenarios, one should take down the surrounding information, skyplot, elevation angle and the configuration, to further exploit their influence on the measurements.

In case of determining unknown base station coordinates, user can use NETPOS product, RTKPOST and Burness software to have real-time and post-processing approaches accordingly, and deploy the experiment following the detail configurations and setups.

Appendix A:
Plots for each control point

For each control point, the three sets of evaluation are conducted base on fix, float and all measurements. For each set of evaluation, time series in each direction, scatter plot in East and North direction, histogram before and after outliers removal procedures are provided.

Control point 1.
Fix solutions:

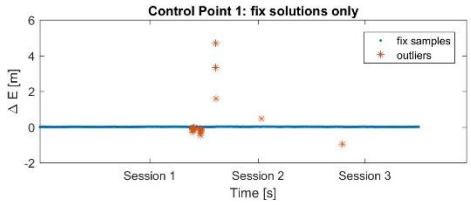

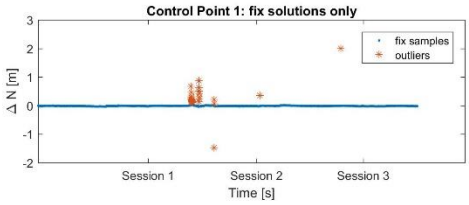

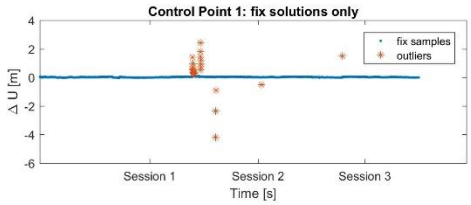

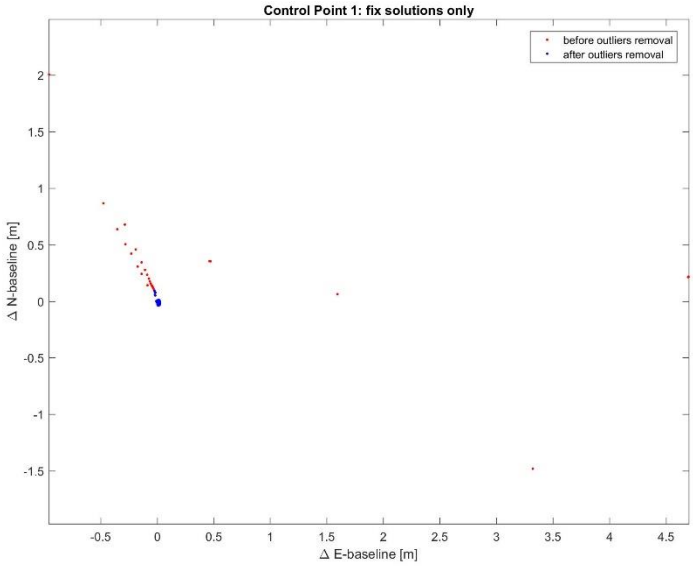

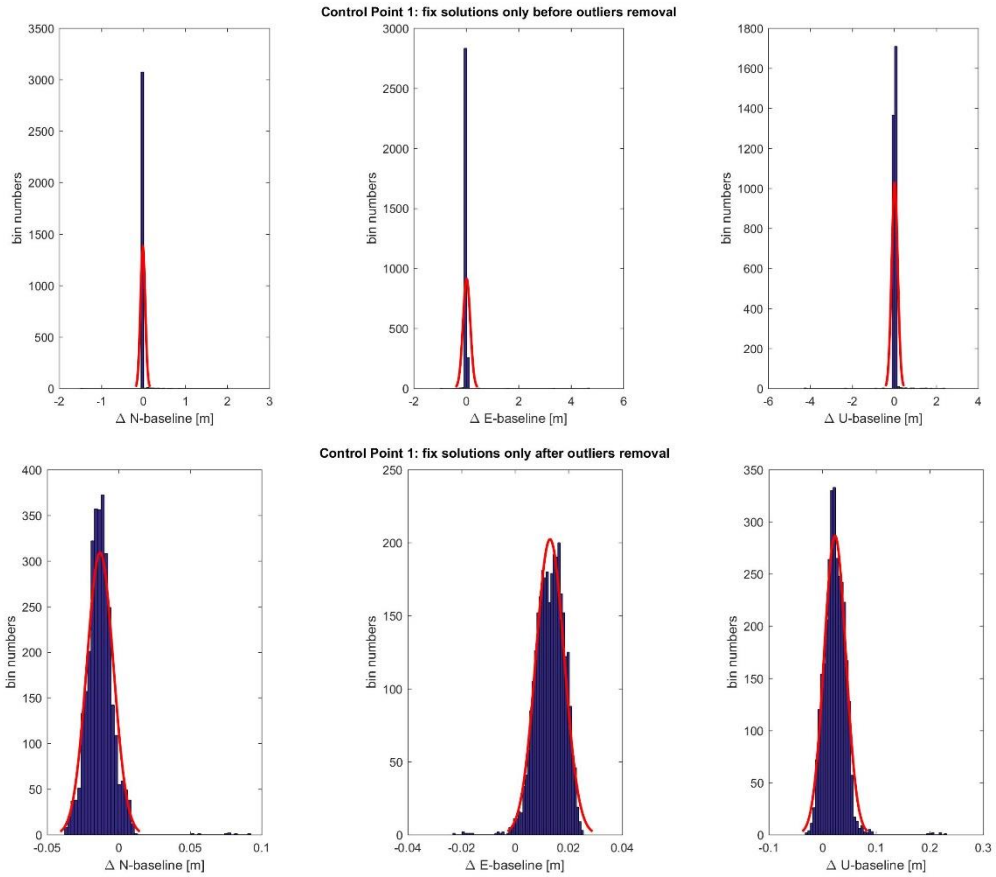

Float solutions:

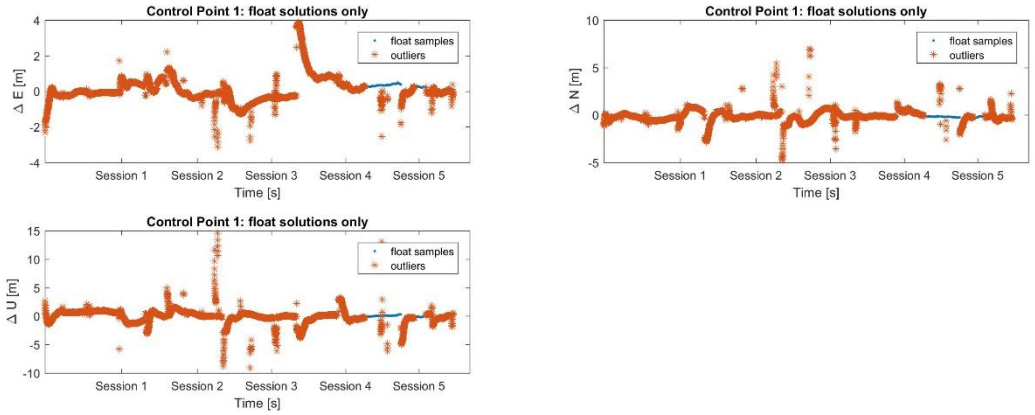

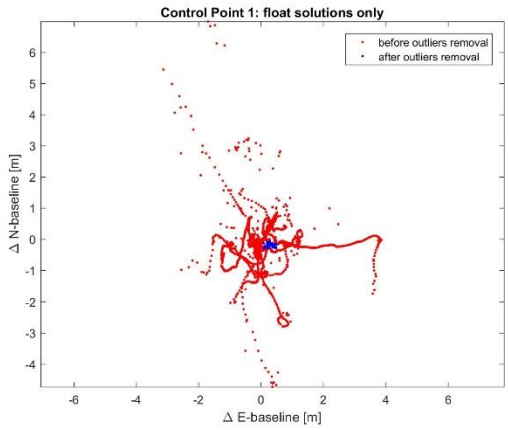

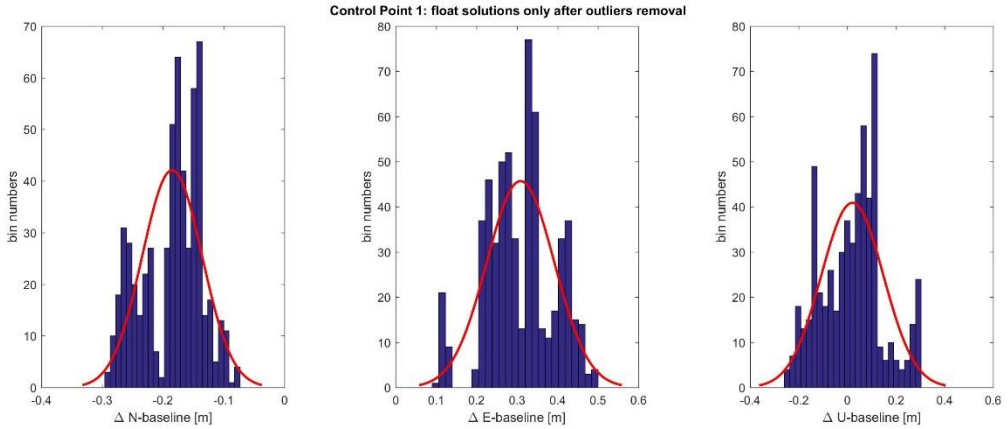

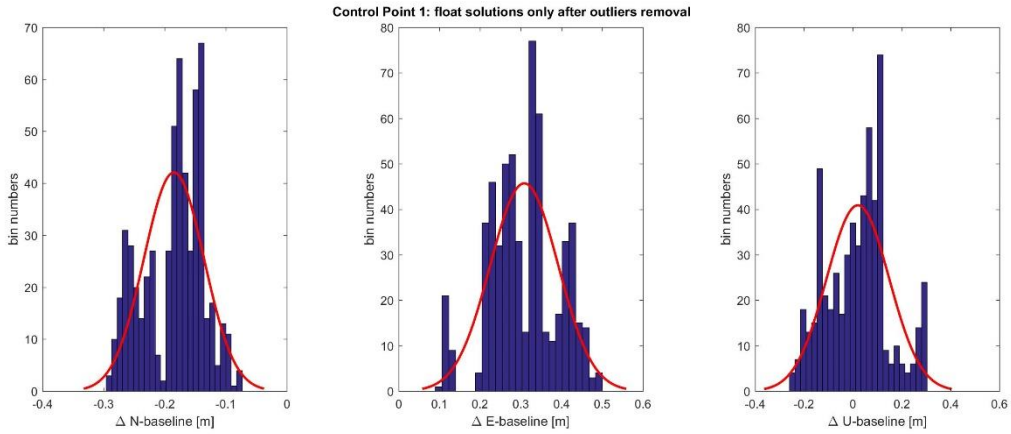

All solutions:

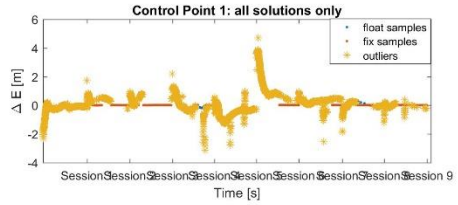
Control Point 1: all solutions only
float samples
fix samples
outliers
Δ E [m]
Time [s]

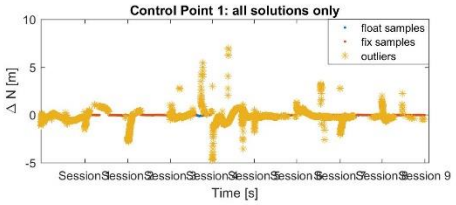
Control Point 1: all solutions only
float samples
fix samples
outliers
Δ N [m]
Time [s]

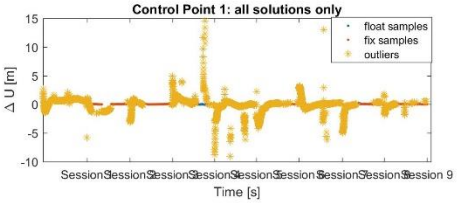
Control Point 1: all solutions only
float samples
fix samples
outliers
Δ U [m]
Time [s]

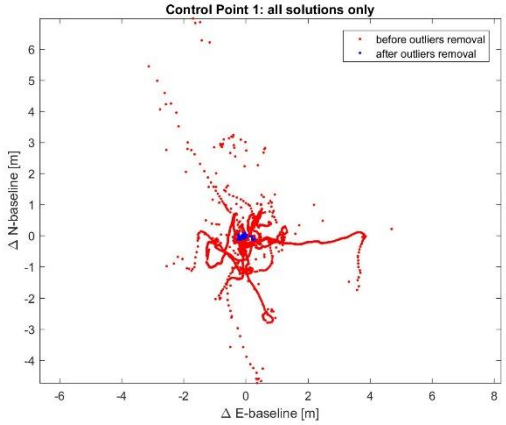
Control Point 1: all solutions only
before outliers removal
after outliers removal
Δ N-baseline [m]
Δ E-baseline [m]

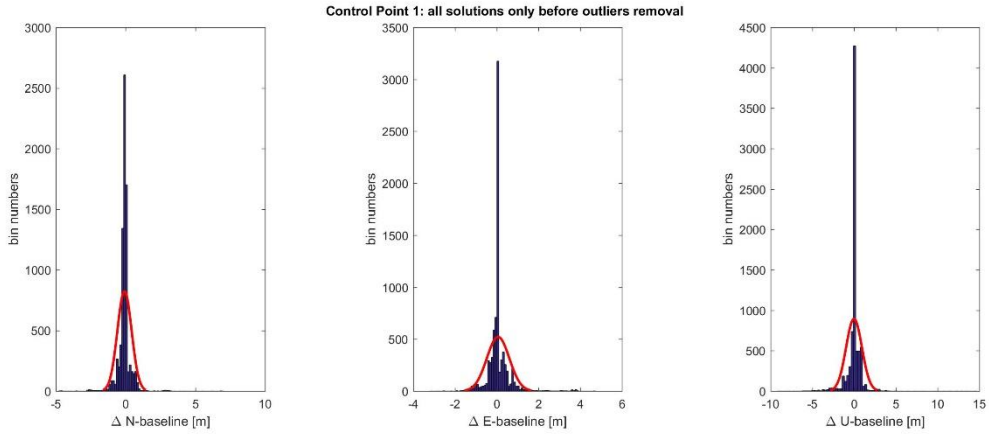
Control Point 1: all solutions only before outliers removal
bin numbers
Δ N-baseline [m]
Δ E-baseline [m]
Δ U-baseline [m]

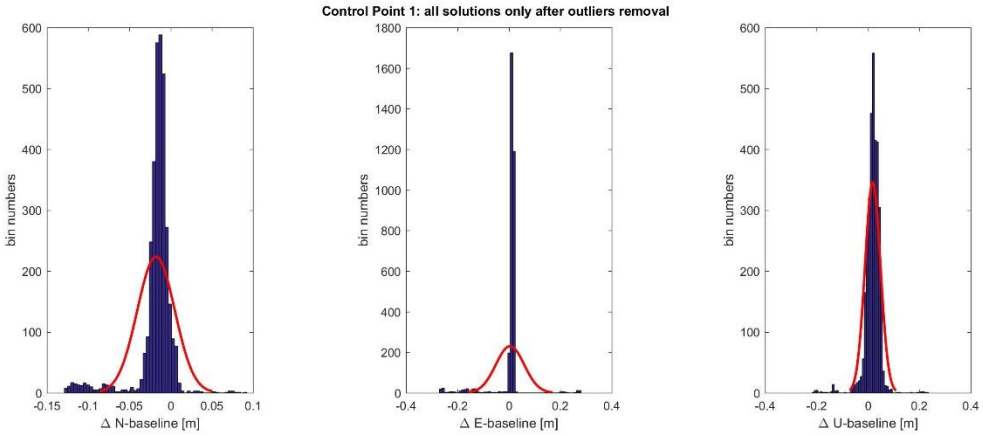

For control point 1, you may wonder in the time series plot, especially for the first session, seems like there should be more reliable solutions than I present, therefore I rescale the y-axis and to have the closer look of the plots. And this time I confine the solutions within 4 meters. One can tell that the 'smooth' curve in previous time series is due to the large scale of the figure, the variations are more evident when have smaller scale of the plot.

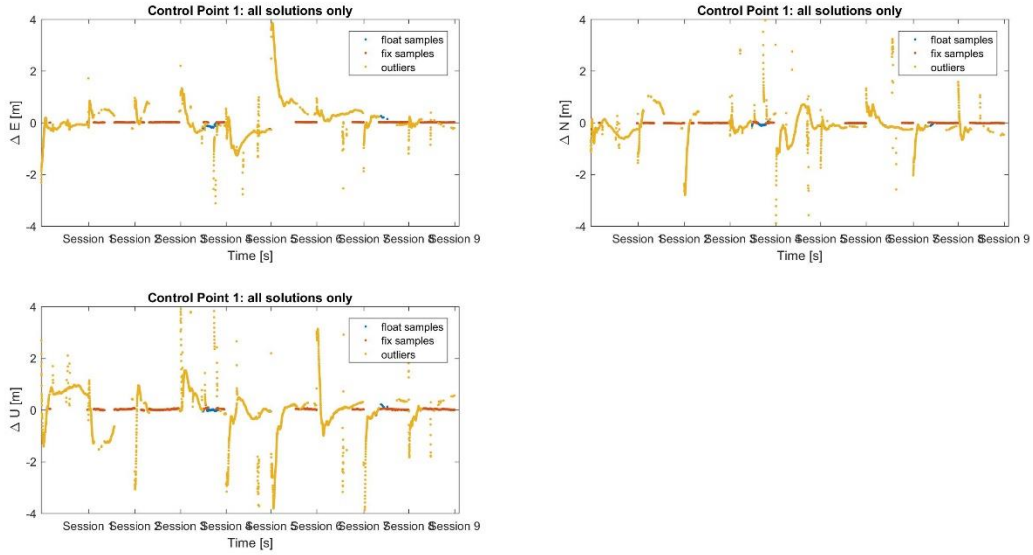

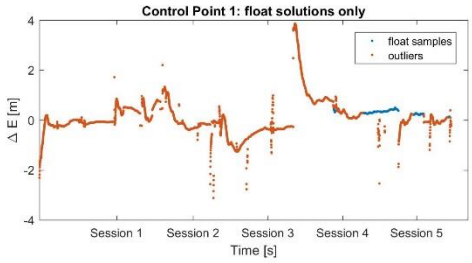

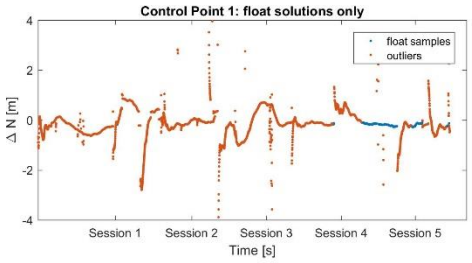

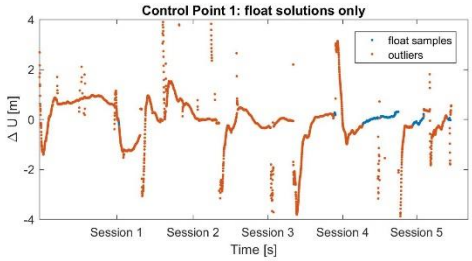

Control point 2.
Fix solutions:

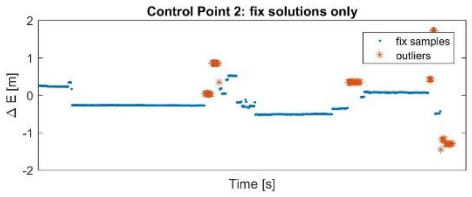

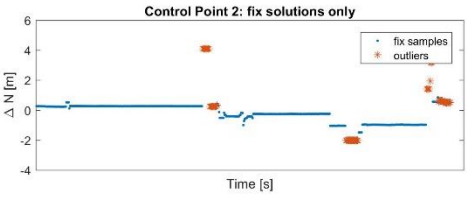

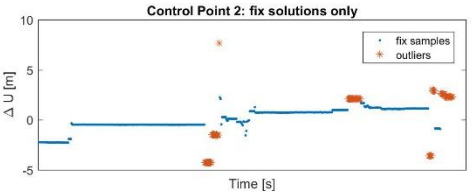

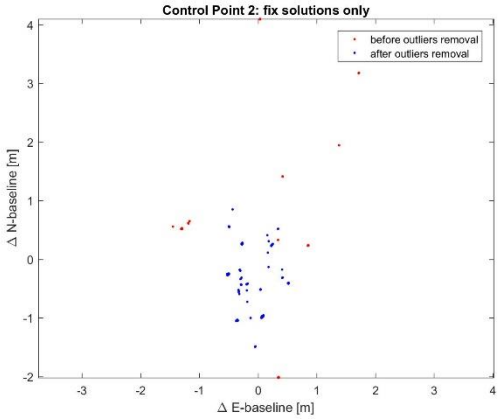

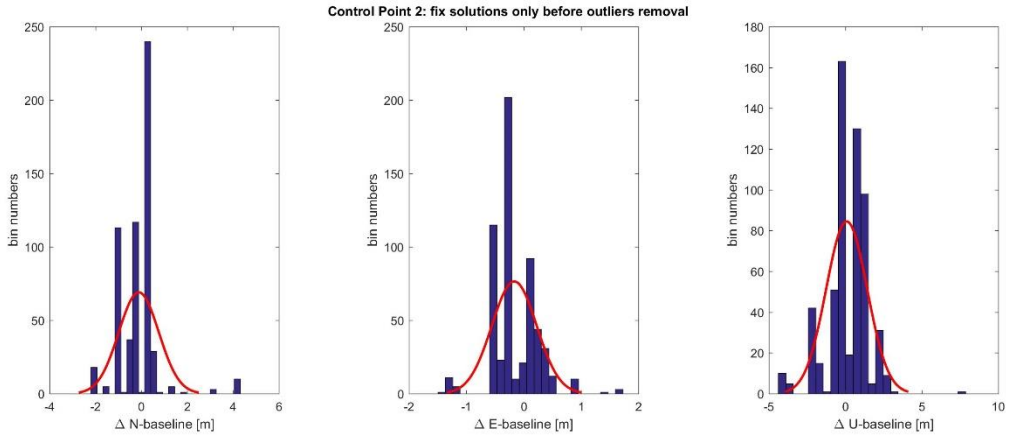

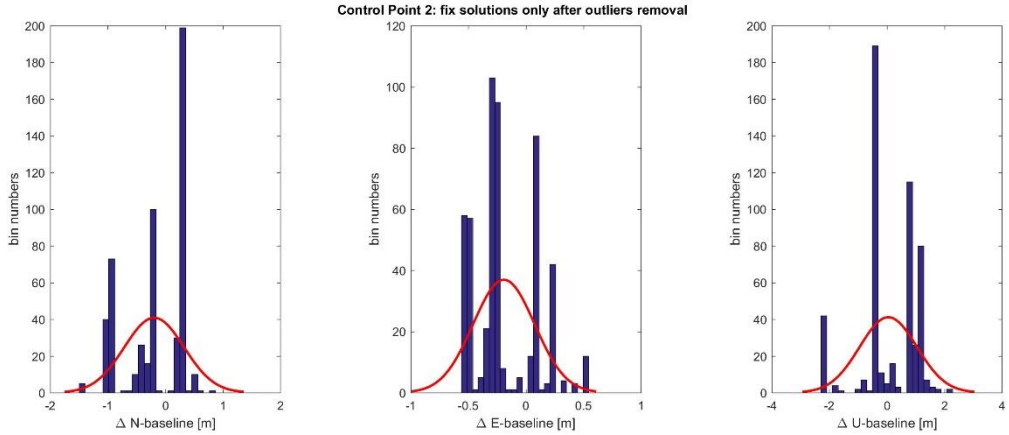

Float solutions:

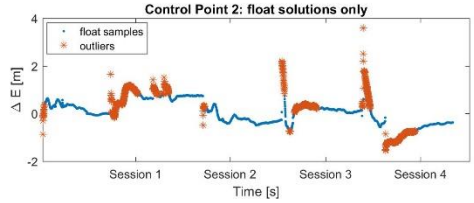

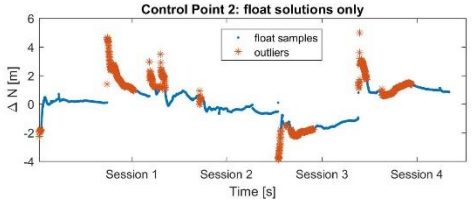

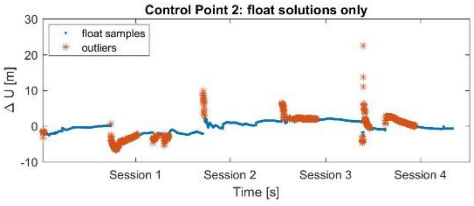

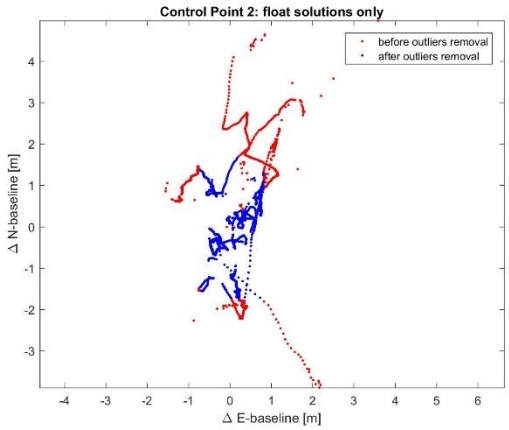

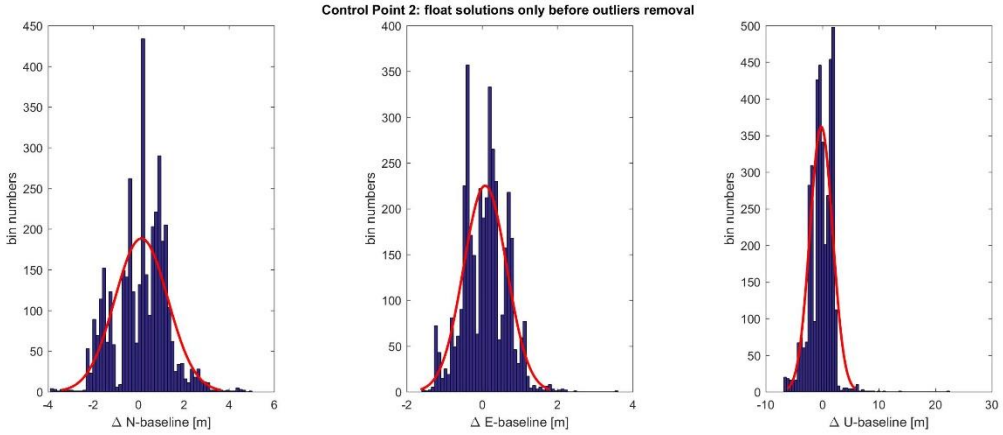

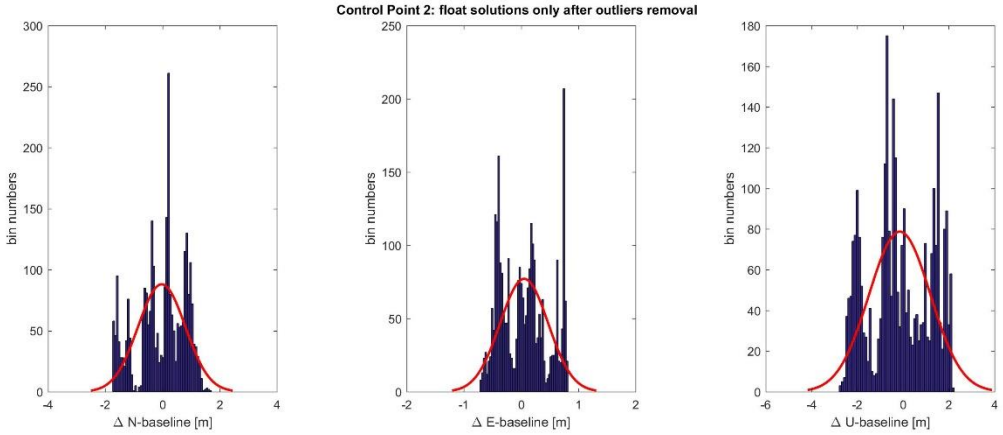

All solutions:

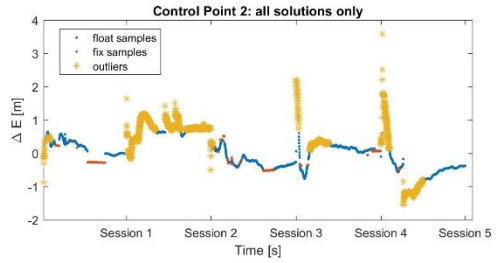
Control Point 2: all solutions only
float samples
fix samples
outliers
Δ E [m]
Session 1
Session 2
Session 3
Session 4
Session 5
Time [s]

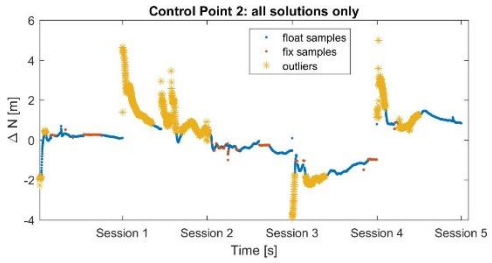
Control Point 2: all solutions only
float samples
fix samples
outliers
Δ N [m]
Session 1
Session 2
Session 3
Session 4
Session 5
Time [s]

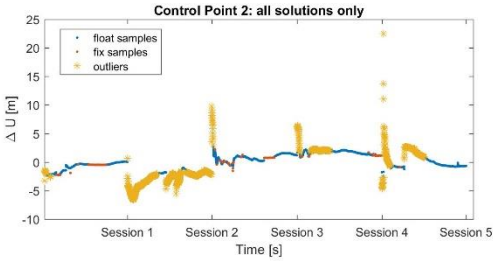
Control Point 2: all solutions only
float samples
fix samples
outliers
Δ U [m]
Session 1
Session 2
Session 3
Session 4
Session 5
Time [s]

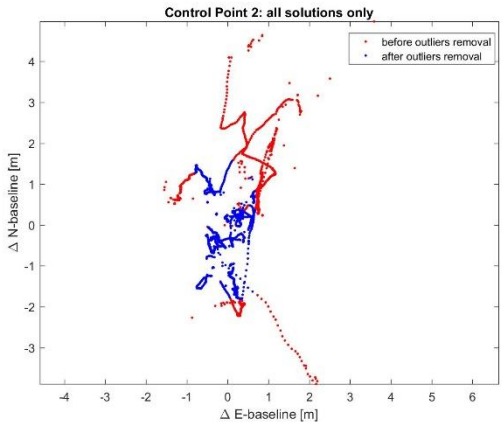
Control Point 2: all solutions only
before outliers removal
after outliers removal
Δ N-baseline [m]
Δ E-baseline [m]

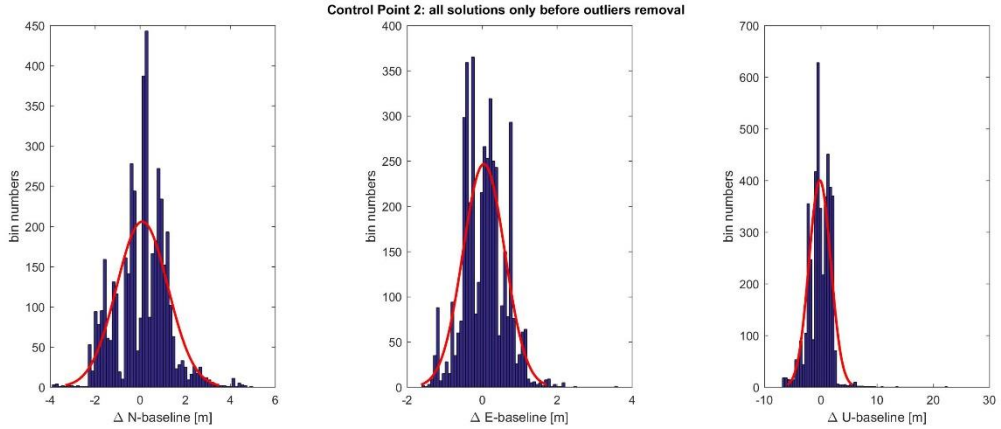
Control Point 2: all solutions only before outliers removal
bin numbers
Δ N-baseline [m]
bin numbers
Δ E-baseline [m]
bin numbers
Δ U-baseline [m]

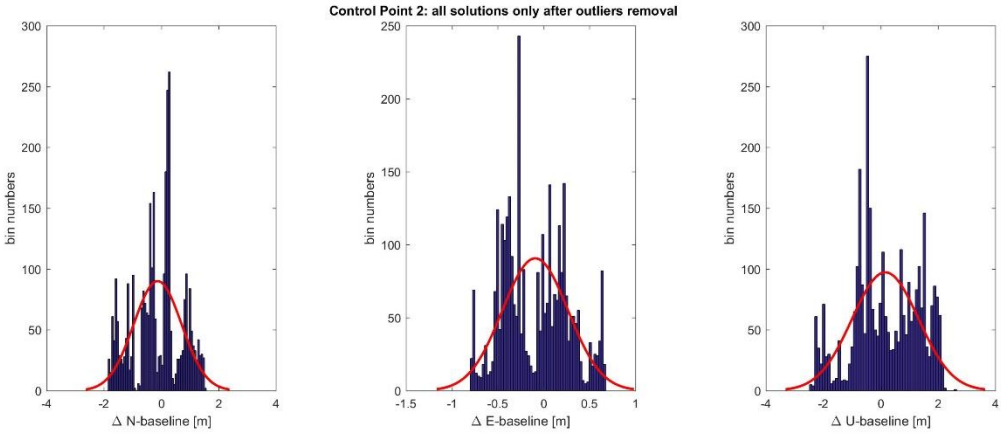

Control point 3.

Fix solutions:

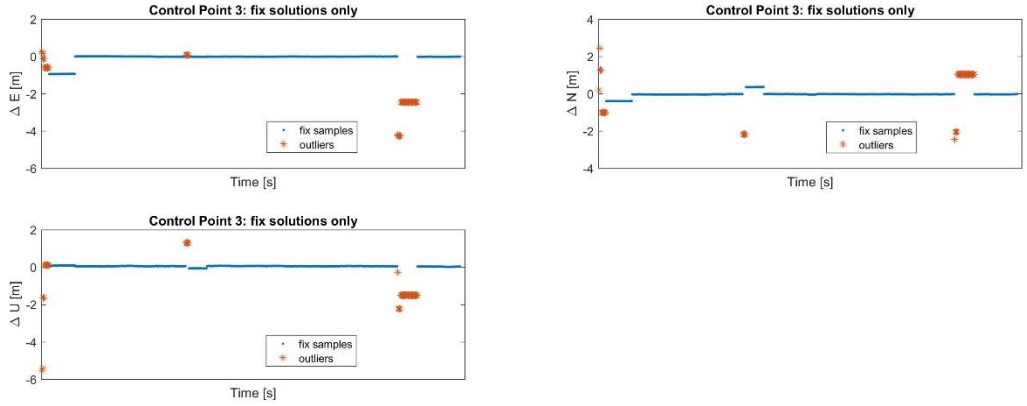

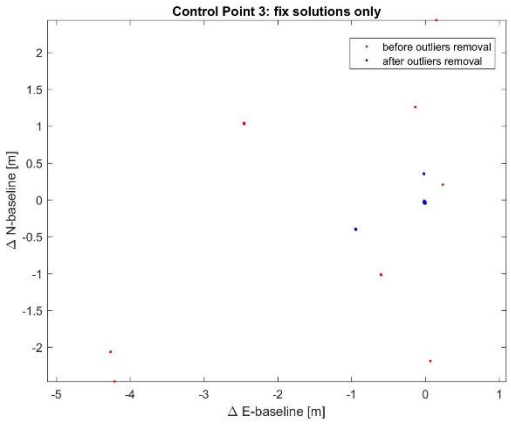

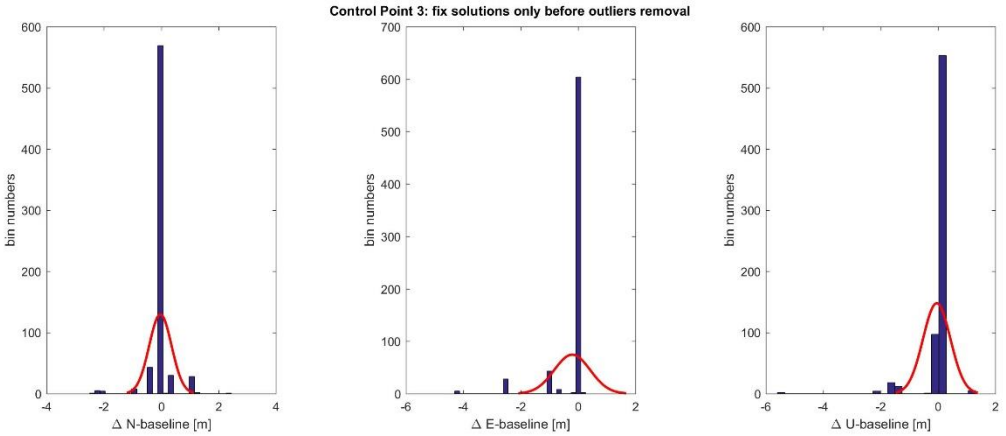

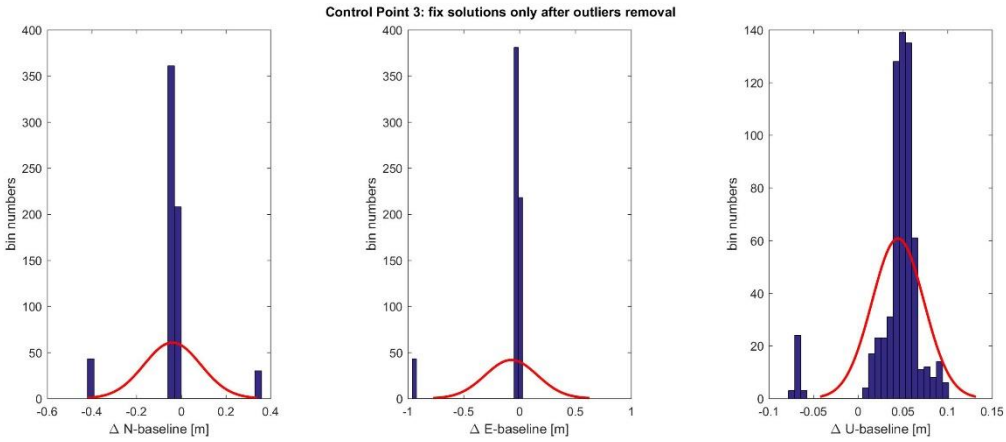

Float solutions:

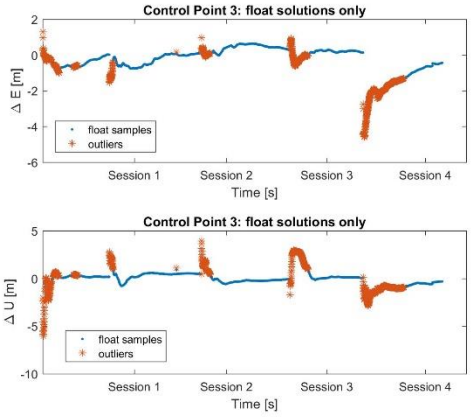

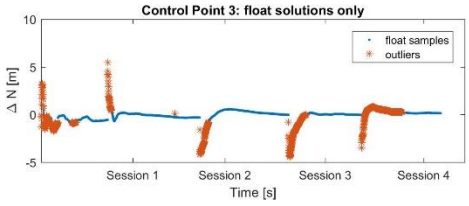

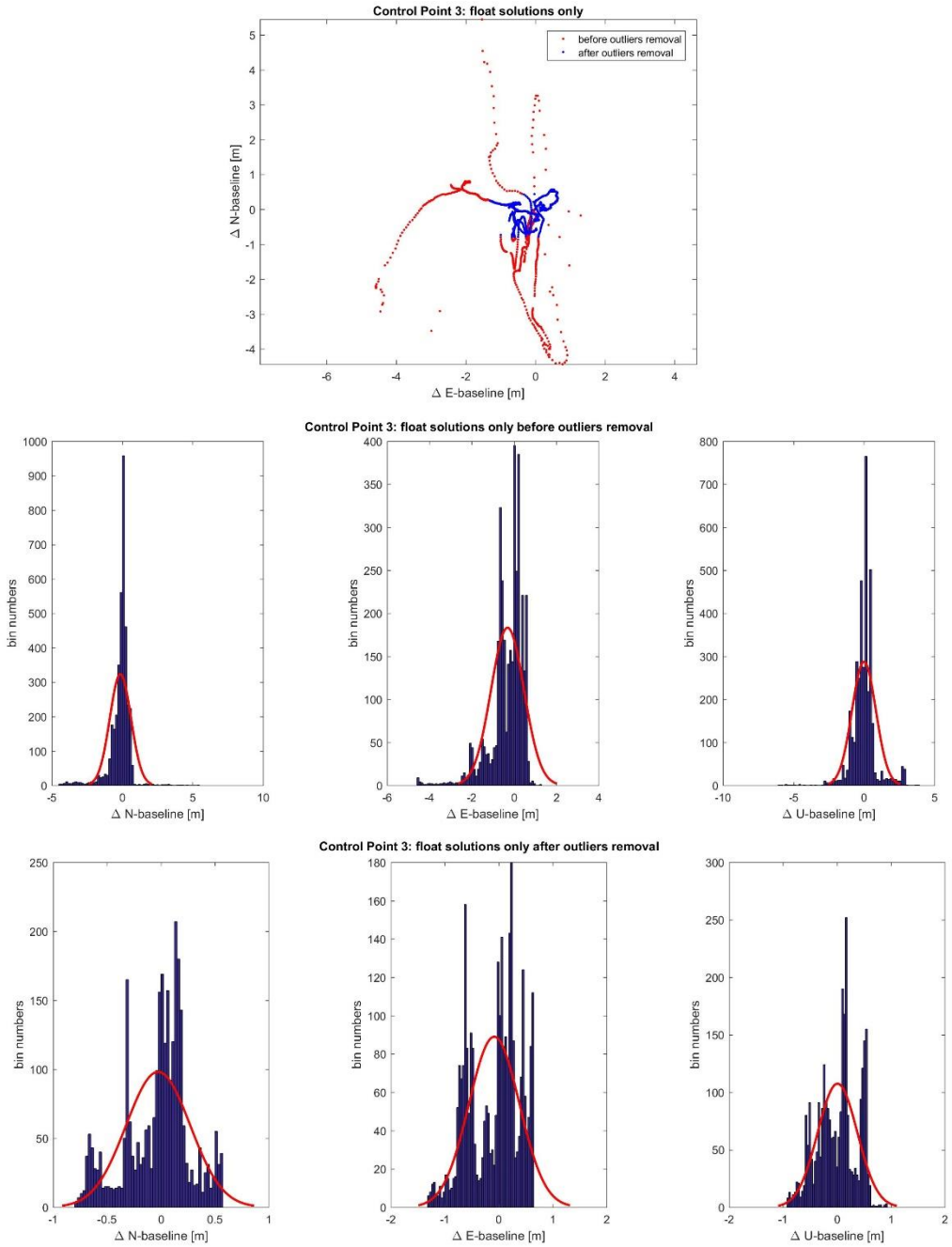

All solutions:

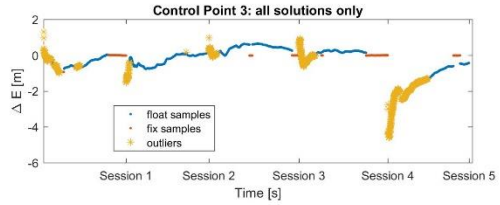
Control Point 3: all solutions only
Δ E [m]
float samples
fix samples
outliers
Session 1
Session 2
Session 3
Session 4
Session 5
Time [s]

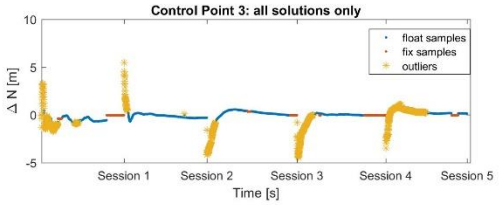
Control Point 3: all solutions only
Δ N [m]
float samples
fix samples
outliers
Session 1
Session 2
Session 3
Session 4
Session 5
Time [s]

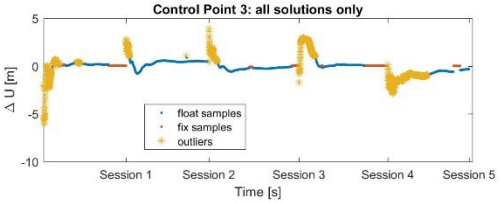
Control Point 3: all solutions only
Δ U [m]
float samples
fix samples
outliers
Session 1
Session 2
Session 3
Session 4
Session 5
Time [s]

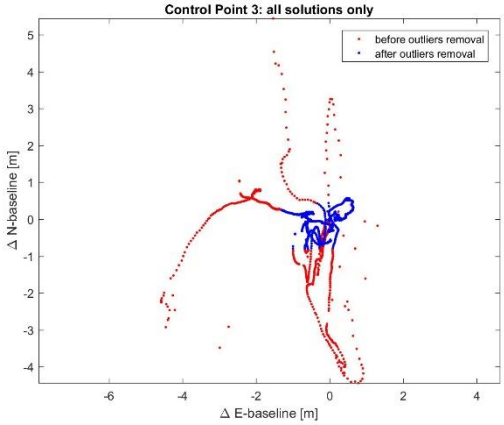
Control Point 3: all solutions only
Δ N-baseline [m]
before outliers removal
after outliers removal
Δ E-baseline [m]

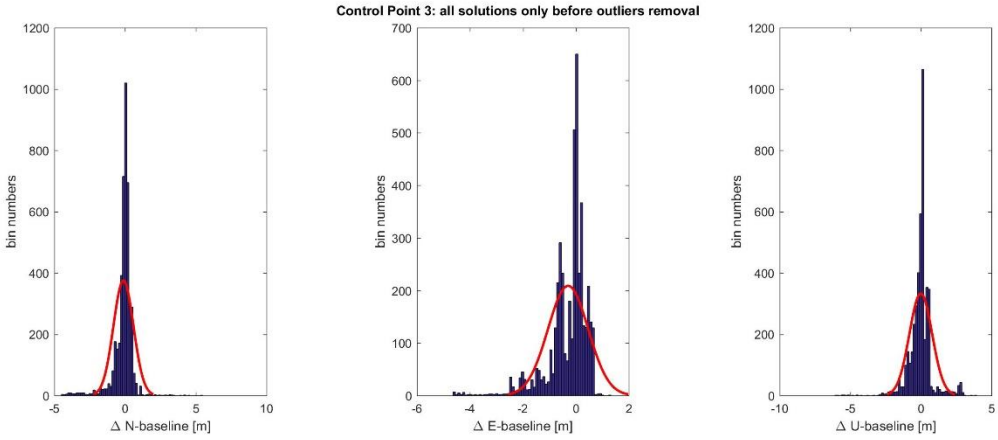
Control Point 3: all solutions only before outliers removal
bin numbers
Δ N-baseline [m]
Δ E-baseline [m]
Δ U-baseline [m]

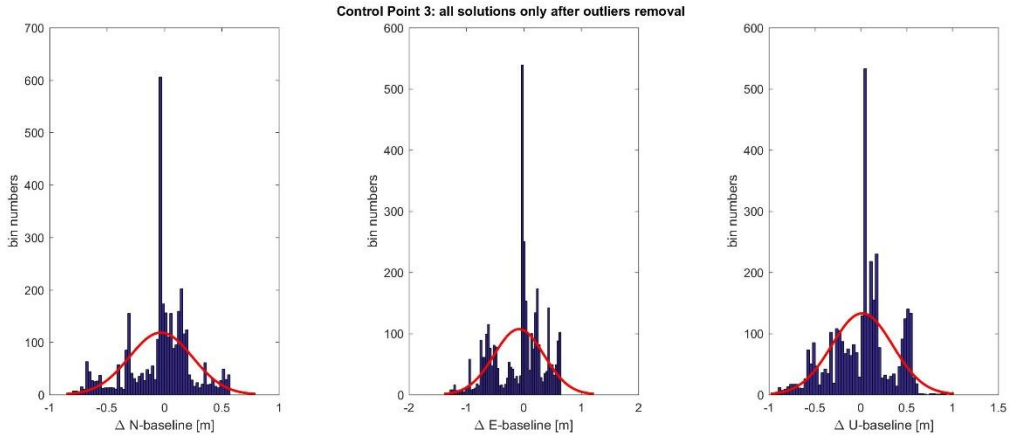

Control point 4.
Fix solutions:

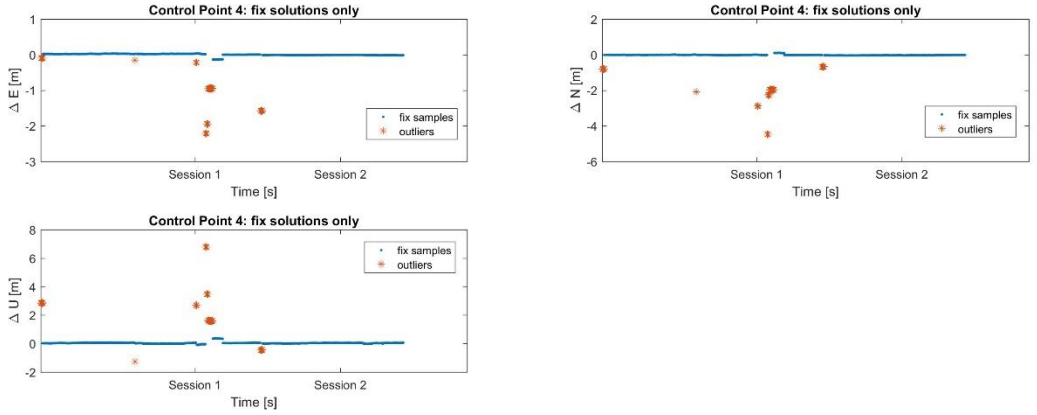

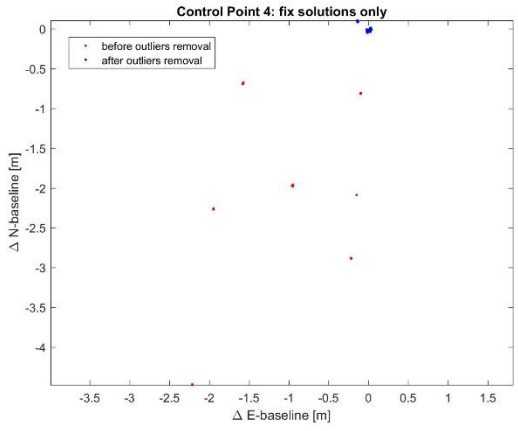

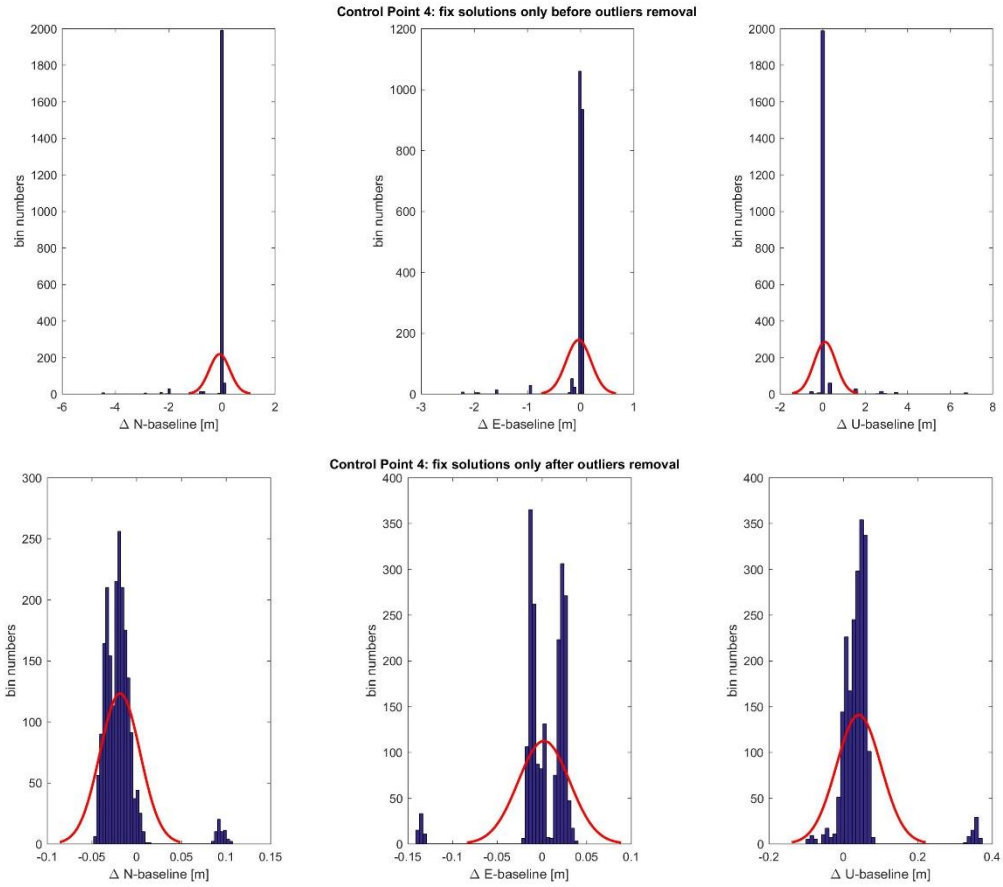

Float solutions:

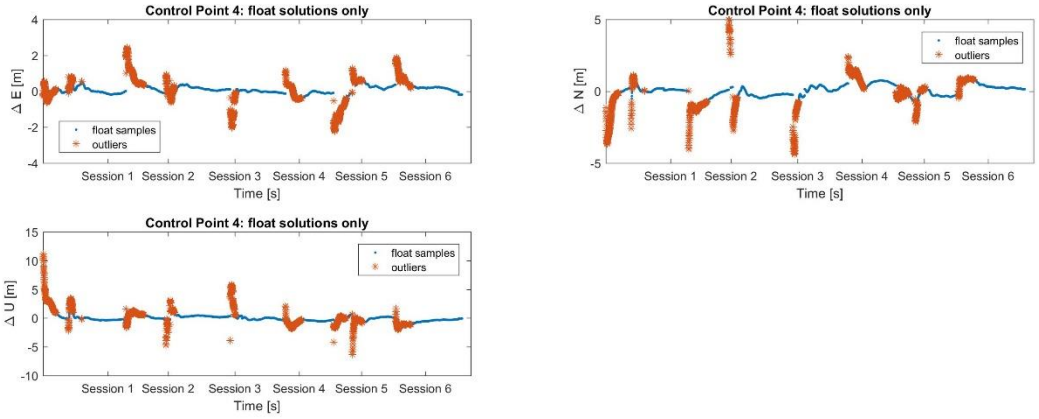

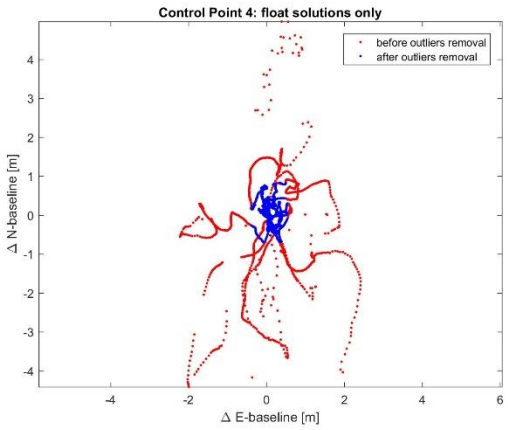

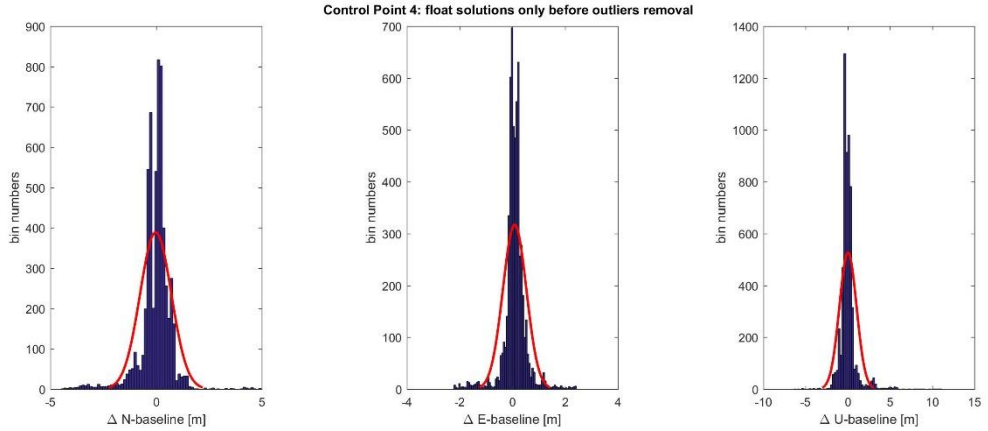

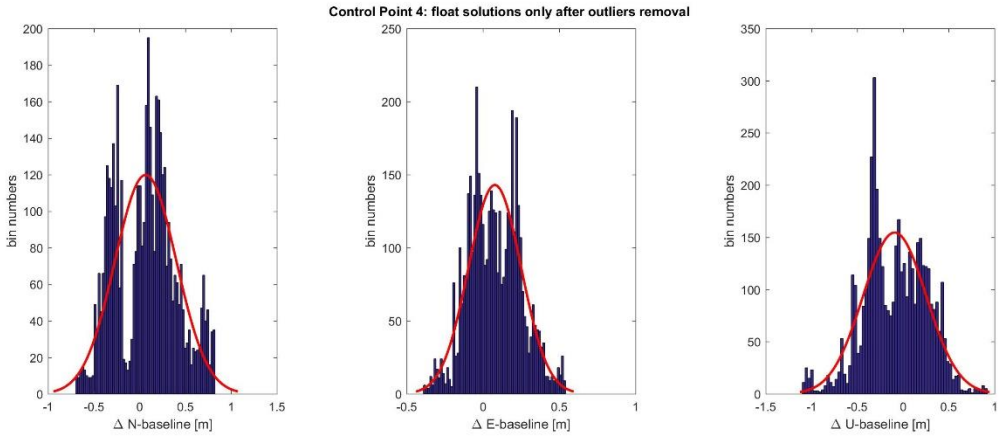

All solutions:

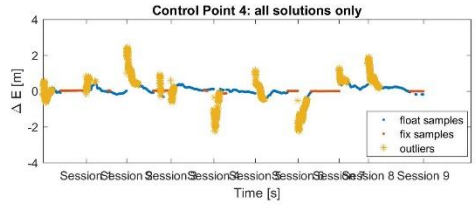
Control Point 4: all solutions only
Δ E [m]
float samples
fix samples
outliers
Session 1 Session 2 Session 3 Session 4 Session 5 Session 6 Session 7 Session 8 Session 9
Time [s]

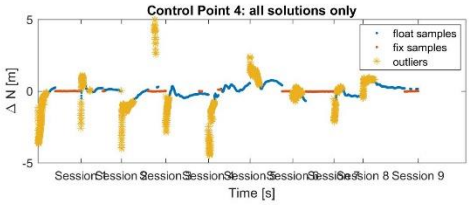
Control Point 4: all solutions only
Δ N [m]
float samples
fix samples
outliers
Session 1 Session 2 Session 3 Session 4 Session 5 Session 6 Session 7 Session 8 Session 9
Time [s]

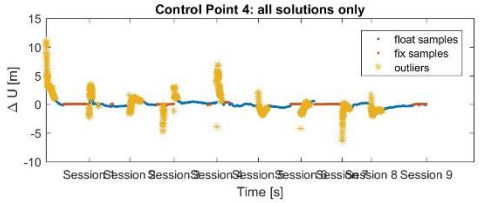
Control Point 4: all solutions only
Δ U [m]
float samples
fix samples
outliers
Session 1 Session 2 Session 3 Session 4 Session 5 Session 6 Session 7 Session 8 Session 9
Time [s]

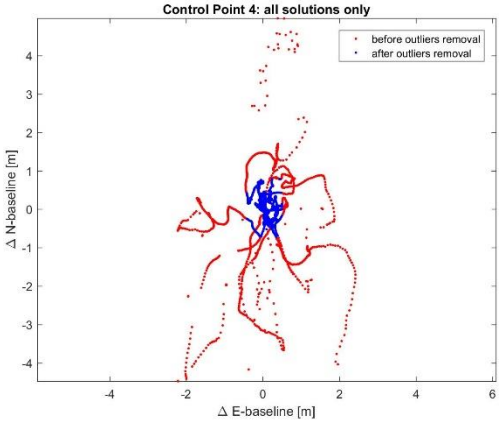
Control Point 4: all solutions only
before outliers removal
after outliers removal
Δ N-baseline [m]
Δ E-baseline [m]

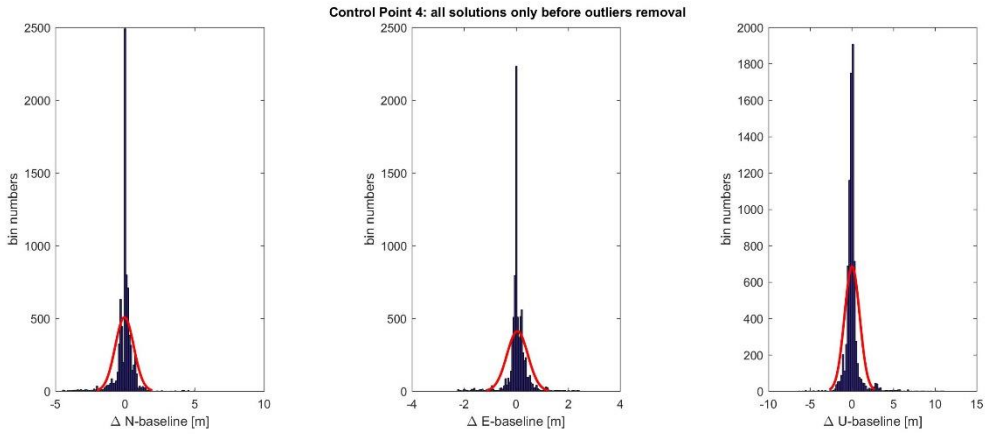
Control Point 4: all solutions only before outliers removal
bin numbers
Δ N-baseline [m]
Δ E-baseline [m]
Δ U-baseline [m]

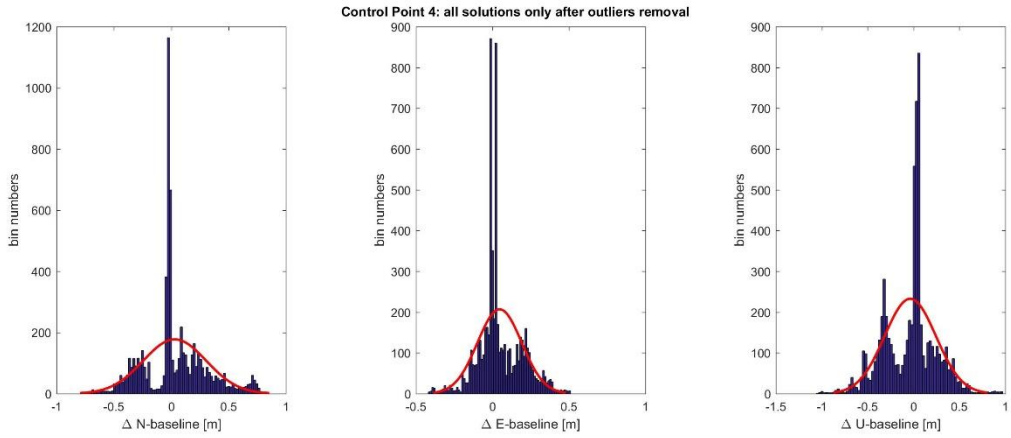

Control point 5.

Fix solutions:

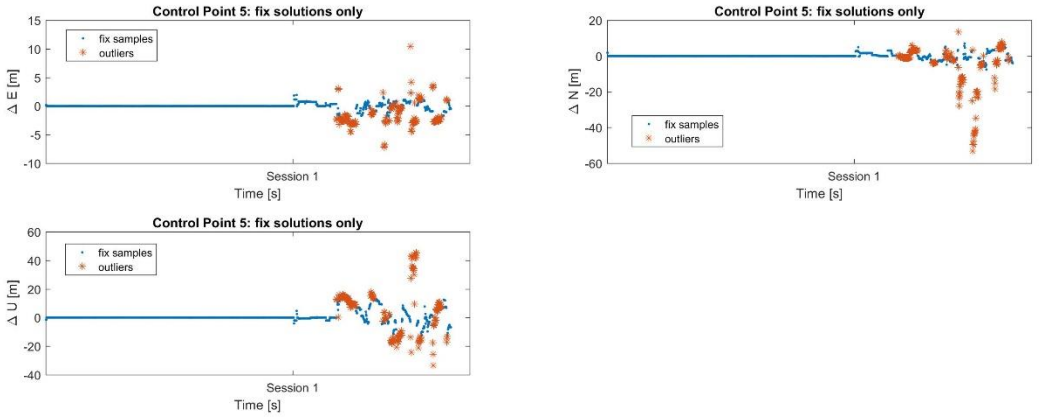

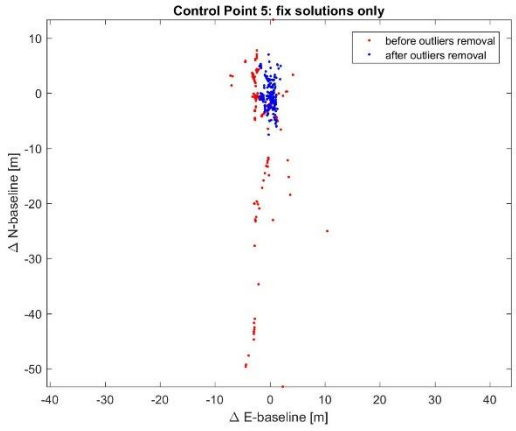

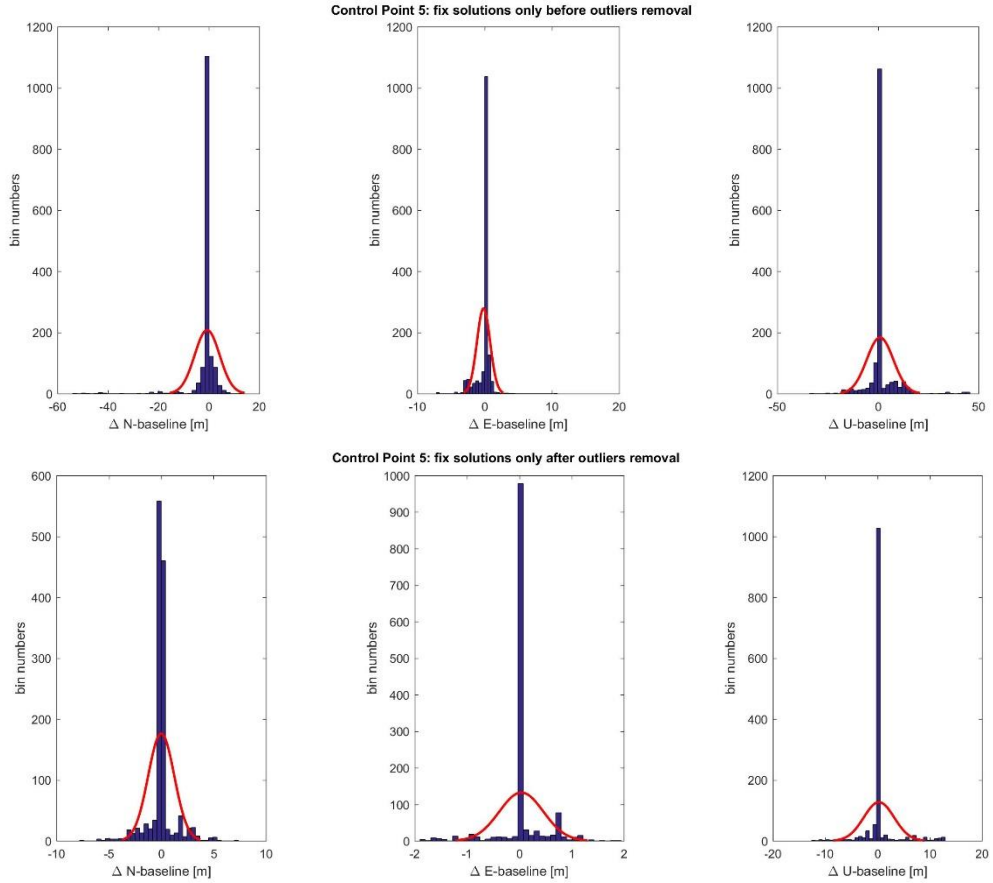

Float solutions:

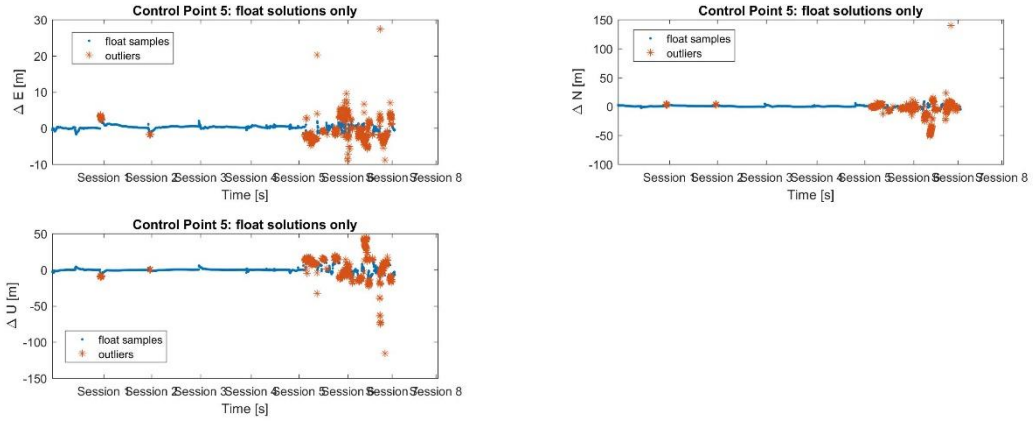

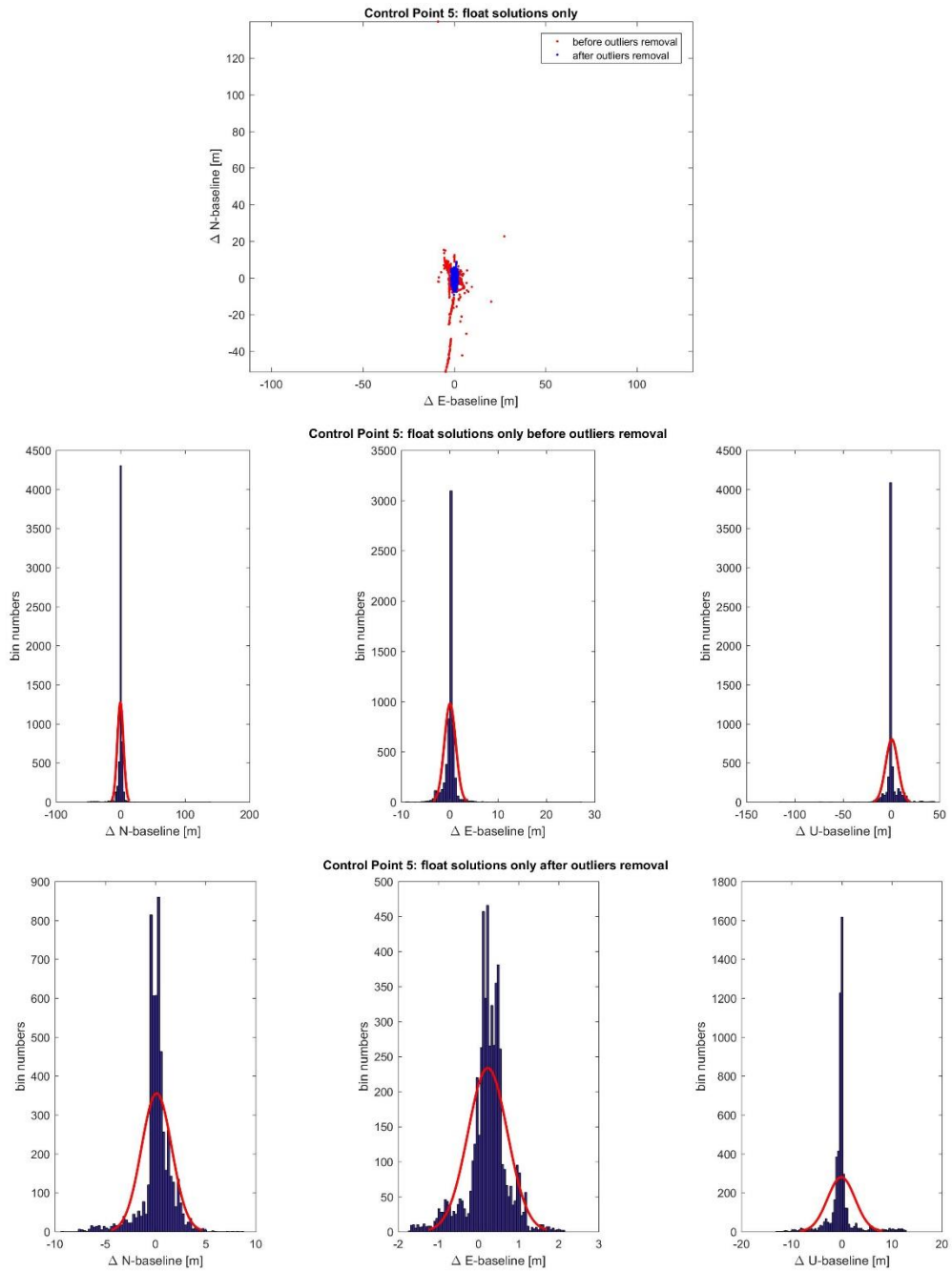

All solutions:

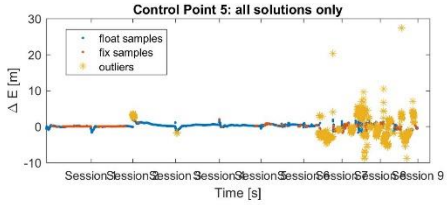
Control Point 5: all solutions only
float samples
fix samples
outliers
Δ E [m]
Time [s]

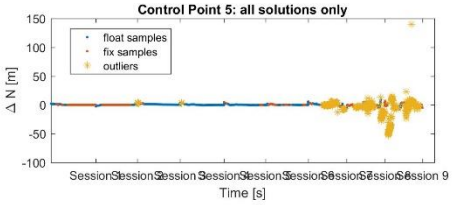
Control Point 5: all solutions only
float samples
fix samples
outliers
Δ N [m]
Time [s]

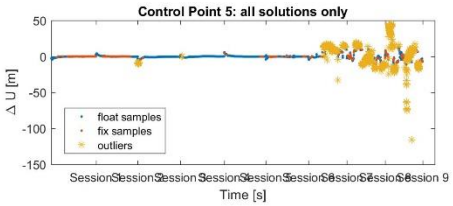
Control Point 5: all solutions only
float samples
fix samples
outliers
Δ U [m]
Time [s]

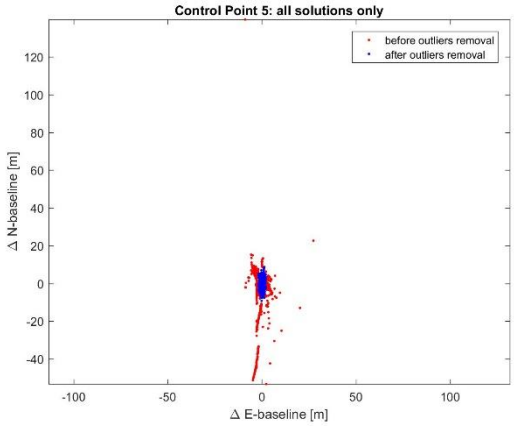
Control Point 5: all solutions only
before outliers removal
after outliers removal
Δ N-baseline [m]
Δ E-baseline [m]

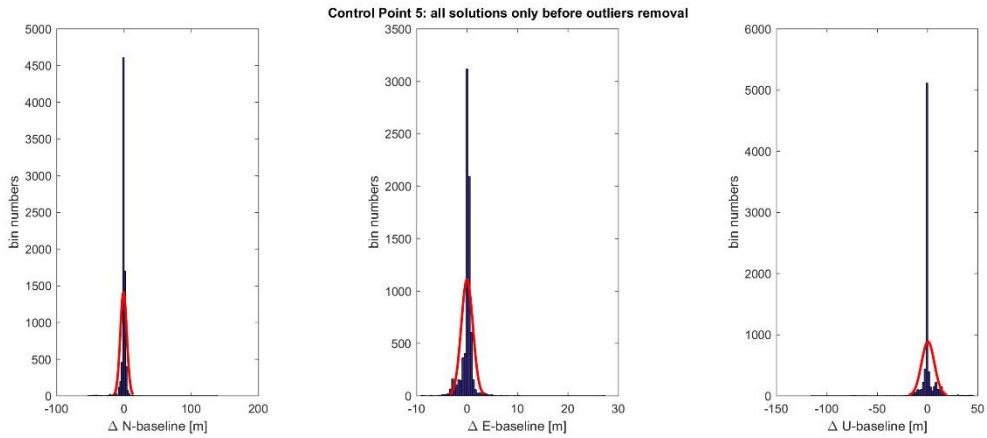
Control Point 5: all solutions only before outliers removal
bin numbers
Δ N-baseline [m]
Δ E-baseline [m]
Δ U-baseline [m]

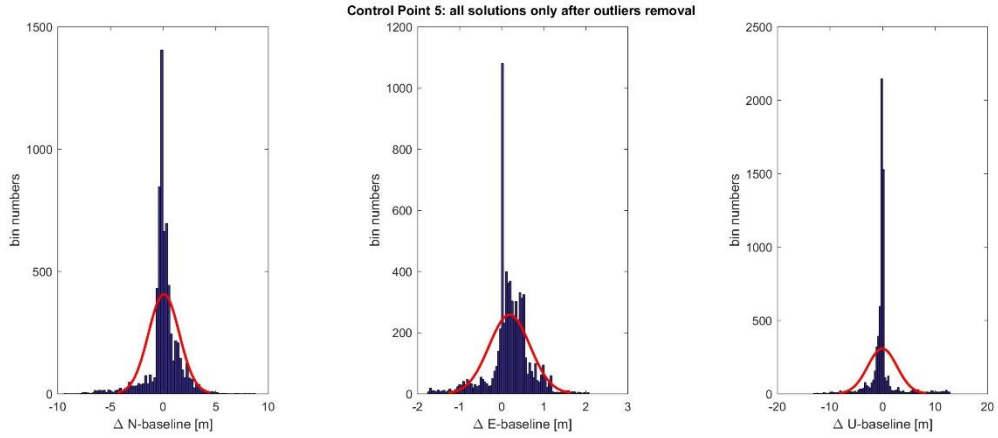

Control point 6.
Fix solutions:

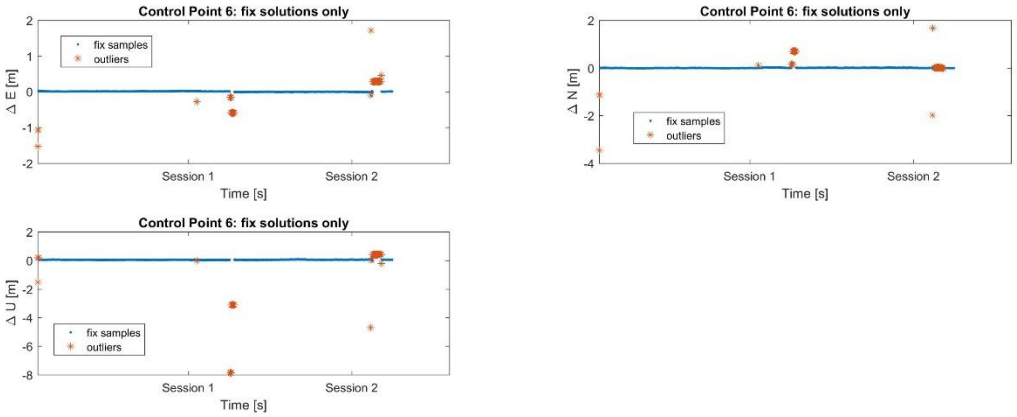

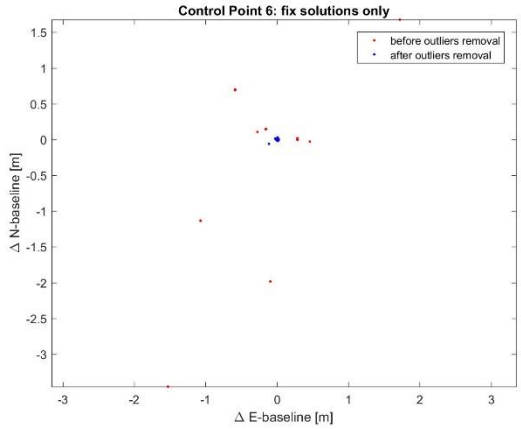

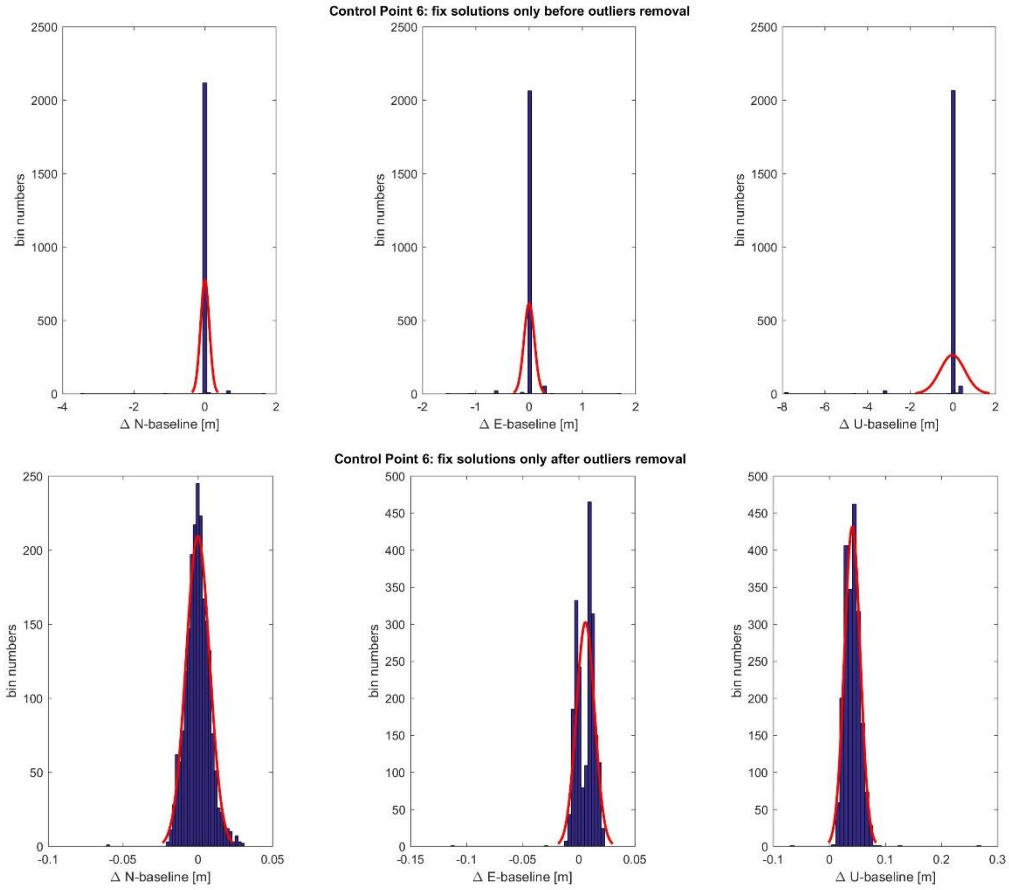

Float solutions:

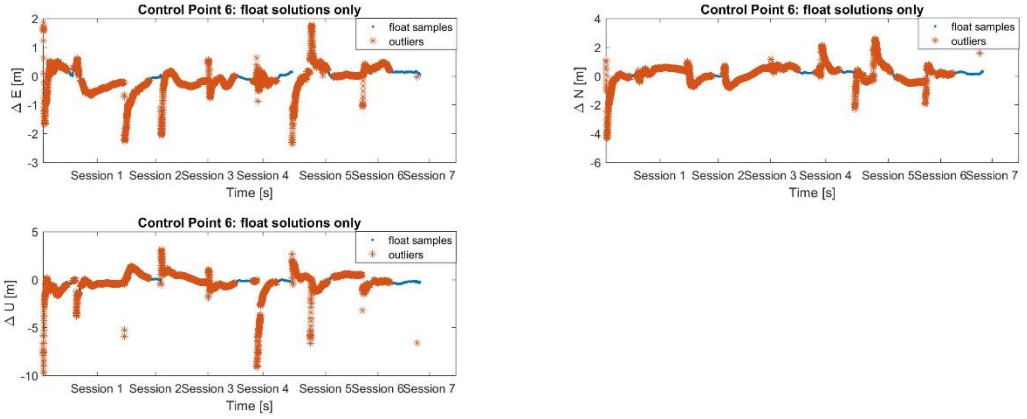

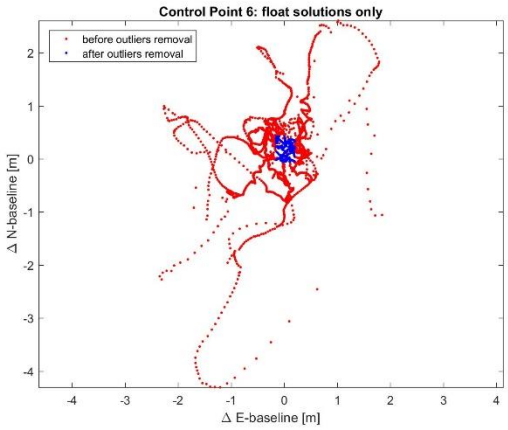

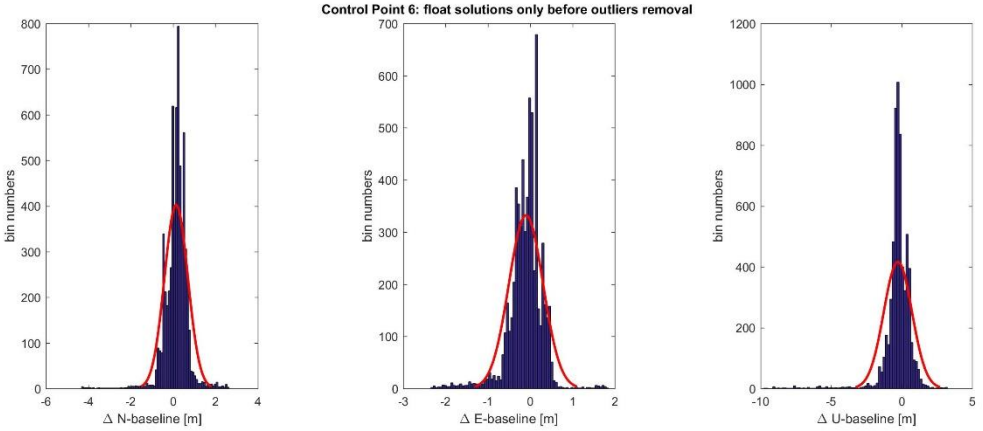

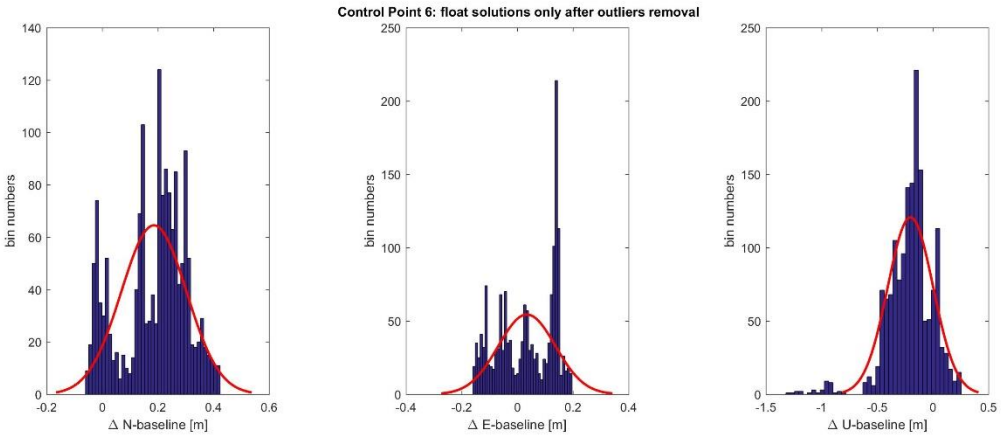

All solutions:

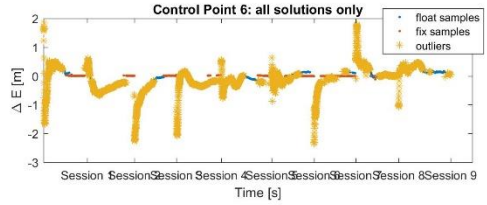
Control Point 6: all solutions only
float samples
fix samples
outliers
Δ E [m]
Session 1Session 2Session 3Session 4Session 5Session 6Session 7Session 8Session 9
Time [s]

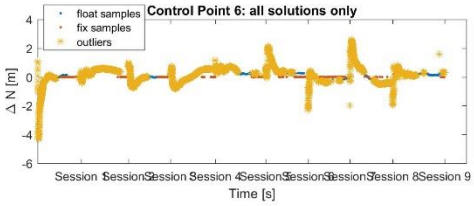
Control Point 6: all solutions only
float samples
fix samples
outliers
Δ N [m]
Session 1Session 2Session 3Session 4Session 5Session 6Session 7Session 8Session 9
Time [s]

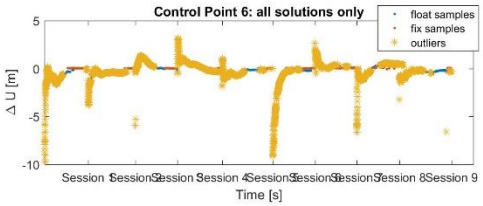
Control Point 6: all solutions only
float samples
fix samples
outliers
Δ U [m]
Session 1Session 2Session 3Session 4Session 5Session 6Session 7Session 8Session 9
Time [s]

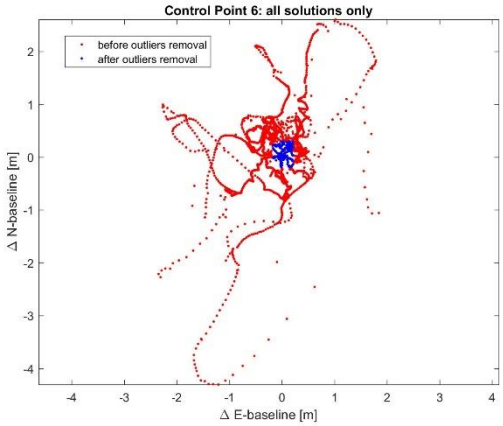
Control Point 6: all solutions only
before outliers removal
after outliers removal
Δ N-baseline [m]
Δ E-baseline [m]

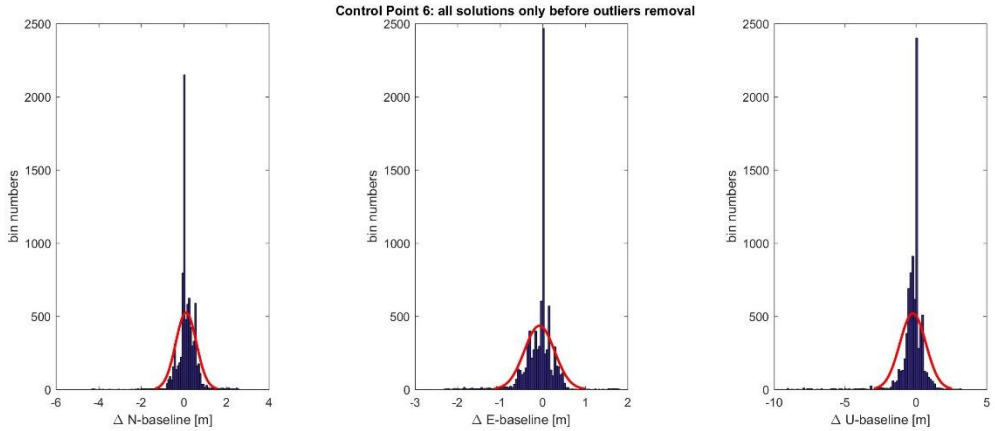
Control Point 6: all solutions only before outliers removal
bin numbers
Δ N-baseline [m]
Δ E-baseline [m]
Δ U-baseline [m]

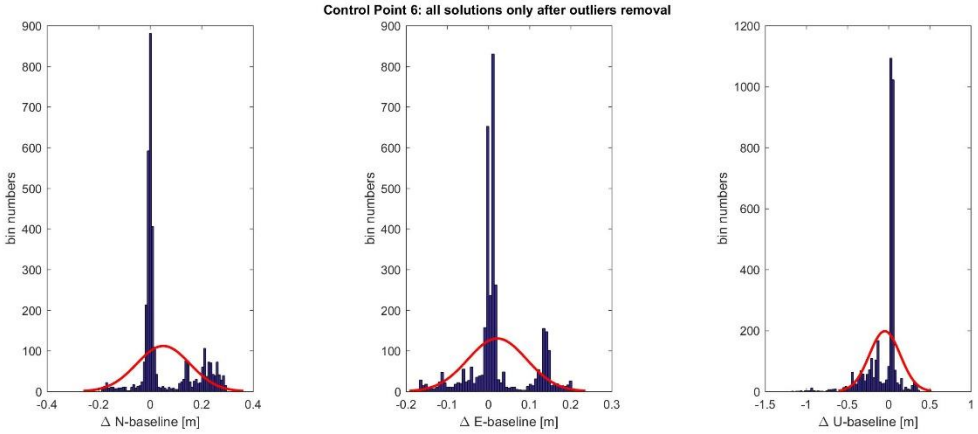
Control Point 6: all solutions only after outliers removal
bin numbers
Δ N-baseline [m]
bin numbers
Δ E-baseline [m]
bin numbers
Δ U-baseline [m]

Appendix B:
Average satellite numbers in view for each session

Sessions	1	2	3	4	5	6	7	8	9
Cp 1	9.8	8.8	8.9	8.5	7.1	7.9	9.1	9.8	8.8
Cp 2	6.3	5.2	5.0	5.0	6.1				
Cp 3	5.2	6.0	6.1	6.5	6.5	6.0			
Cp 4	7.0	7.0	7.0	6.6	6.0	8.7	8.9	8.5	8.1
Cp 5	8.5	8.0	7.0	6.9	5.7	7.0			
Cp 6	6.9	8.4	9.0	8.8	8.0	8.7	8.3	7.7	7.1

Appendix C:
TTSF for each session

Unit: seconds

Sessions	**1**	**2**	**3**	**4**	**5**	**6**	**7**	**8**	**9**
Cp 1	*n/a*	505	275	*n/a*	*n/a*	708	*n/a*	458	250
Cp 2	462	*n/a*	550	*n/a*	*n/a*				
Cp 3	683	*n/a*	*n/a*	704	*n/a*				
Cp 4	365	*n/a*	563	*n/a*	*n/a*	675	279	*n/a*	881
Cp 5	695	*n/a*	*n/a*	*n/a*	*n/a*	*n/a*	*n/a*	*n/a*	*n/a*
Cp 6	611	824	614	*n/a*	*n/a*	*n/a*	*n/a*	*n/a*	*n/a*

Acknowledgement:

I would like to thank Ir. Lennard Huisman, who provided an opportunity of conducting the experiment, and gave instructions and explanations on how to use NETPOS product. I am also grateful to Wim Witteveen, who showed me the experiment setup in practice, deployment of the control point, taking the measurements and the documents I need in part III. I also would like to thank Dr. Ir. Peter de Bakker, who provided insight and expertise that greatly assisted to modify the algorithm of the model. I also would like to show my gratitude to Dr. Ir .C.C.J.M Tiberius for giving me the introduction of background knowledge of the experiment, he and Peter provided me comments and suggestions in conducting the experiment.

References

Bolting, J., Defa, F., & Moschetta, J. (2013). Differential GPS for small UAS using consumer-grade single-frequency receivers, (September), 17–20.

Chen, K., & Gao, Y. (2005). Real-Time Precise Point Positioning Using Single Frequency Data. *Proceedings of the 18th International Technical Meeting of the Satellite Division of The Institute of Navigation (ION GNSS 2005)*, 1514–1523. Retrieved from http://www.ion.org/search/view_abstract.cfm?jp=p&idno=6350

Douša, J., Filler, V., Kostelecký, J., Kostelecký, J., & Šimek, J. (2010). EUREF-Czech-2009 Campaign, (April).

IGS. (2017). About. Retrieved from http://www.igs.org/about#Organization

Karolina SZAFRANEK *, J. B. and M. F., & Kaliskiego. (2013). GNSS Reference Solution For Permanent Station Stability Monitoring And Geodynamical Investigations: The ASG-EUPOS case study. *Acta Geodyn. Geomater*, *10*(1), 67–75.

Pesyna, K. M., Heath, R. W., & Humphreys, T. E. (2015). Accuracy in the palm of your hand: Centimeter positioning with a smartphone-quality GNSS antenna. *GPS World*, *26*(2), 16–31.

Qu, M. (2012). *Experimental Studies of Wireless Communication and Gnss Kinematic Positioning Performance in High-Mobility Vehicle Environments*. Queensland University of Technology.

Sneeuw, N., Novák, P., Crespi, M., & Sansó, F. (2012). VII Hotine-Marussi Symposium on Mathematical Geodesy: Proceedings of the Symposium in Rome, 6-10 June, 2009. *International Association of Geodesy Symposia*, *137*. http://doi.org/10.1007/978-3-642-22078-4

Stempfhuber, W., & Buchholz, M. (2011). High-End and Low-Cost RTK GNSS in Machine Control and Precision Farming Applications. *FIG Working Week 2011, Bridging the Gap between Cultures*, (May), 5168.

Takasu, T., & Yasuda, A. (2004). Evaluation of RTK-GPS Performance with Low-cost Single-frequency GPS Receivers. International Symposium on GPS/GNSS 2008.

Takasu, T., & Yasuda, A. (2009). Development of the low-cost RTK-GPS receiver with an open source program package RTKLIB. *International Symposium on GPS/GNSS*, 4–6.

Takasu, T., & Yasuda, A. (2013). RTKLIB ver. 2.4.2 Manual, (C), 181. Retrieved from http://www.rtklib.com/rtklib.htm

Trimble.Inc. (n.d.). Critical factors affecting RTK accuracy. Retrieved from http://www.trimble.com/OEM_ReceiverHelp/V4.44/en/PositionModes_CriticalFactorsRTK.html

Ublox. (2016). *GNSS evaluation software for Windows*.